UNIVERSITY OF KWAZULU-NATAL

# Ultrafiltration of lignin from black liquor obtained from a South African Kraft mill

By

Paul Thabo Kekana

213565352

A dissertation submitted in partial fulfillment of the requirements for the degree of

MASTER OF SCIENCE IN ENGINEERING: CHEMICAL ENGINEERING

In the School of Engineering

Discipline of Chemical Engineering

Supervisor: Prof. Bruce B. Sithole

Co-Supervisors: Prof Deresh Ramjugernath, Prof Lingam Pillay

March 2015

# DECLARATION

This research has not been previously accepted for any degree and is not being currently considered for any other degree at any other university.

I declare that this Dissertation contains my own work except where specifically acknowledged

Paul Thabo Kekana 213565352

Signed……  ……

Date…16 March 2015

# ACKNOWLEDGEMENTS


- I thank God Almighty for making it possible for me complete this project
- I would like to thank my supervisor, Professor Bruce B. Sithole for encouraging me to enroll for postgraduate studies and for his patience and guidance during the course of the project.
- I would like to thank my co-supervisors, Professor Deresh Ramjugernath and Professor Lingam Pillay for their support and input during the course of the project.
- I thank the CSIR and University of KwaZulu-Natal for awarding me a postgraduate scholarship as well as providing office and laboratory and work facilities
- I appreciate the support I received from my family throughout the study period
- I wish to thank staff members and fellow postgraduate students from the Forestry and Forest Products Research Centre

# ABSTRACT

This study focused on investigating the possibility of extracting lignin from black liquor generated from South African Kraft mill black liquors. Although ultrafiltration has been applied successfully and widely to extract lignin from black liquor it was expedient to conduct this study and apply the technique to black liquor generated from a South African Kraft mill since the structure and the composition of lignin varies mainly as a function of their origin (softwoods, hardwoods or herbaceous crops) but also of several factors such as growth conditions, harvesting and drying of the lignocellulosic biomass. The main hypothesis in this study therefore is that ultrafiltration could be used effectively as a technique to extract lignin from black liquor generated from South African Kraft mill black liquor. In addition, simulations can be performed to elucidate the fouling mechanism by which the flux decline experimental data conforms to.

The test protocol in this work commenced with finding the optimum membrane cut-off size at which the retention of lignin and decline in flux could be studied. The ultrafiltration feasibility tests were performed later in batch mode. In this study batch ultrafiltration tests were conducted to investigate the effects of operating pressure, stirring rate and feed concentration on the extent of lignin retention and permeate flux. Results showed that retention of lignin increased with increase in operating pressure, feed concentration and stirring rate but decreased with increase in molecular cut-off size of the membrane. Permeate flux on the other hand increased with an increase in pressure, stirring rate and molecular cut-off size of the membrane but decreased with increase in feed concentration. The flux decline experimental data was modelled by applying the solute mass balance for a stirred cell and by assuming that fouling mechanism is described by the intermediate blocking model.

The main achievements in this study are:

- The extraction of lignin from black liquor was successfully carried out by ultrafiltration on a bench scale using a stirred cell and extraction efficiencies as high as 86% could be achieved depending on the experimental conditions
- The flux decline results were modelled by applying the experimental data to the intermediate blocking model

This study was concluded with recommendations to perform more tests in order to

- Study the retention of lignin by ultrafiltration using ceramic membranes in a continuous pilot plant setup
- Investigate generation of activated carbon from the precipitated lignin
- Characterize the activated carbons and compare them to commercial samples
- study the potential of using the activated for water purification
- Develop models for the activity and performance of the carbons.

# TABLE OF CONTENTS

# LIST OF TABLES

**PAGE**

## LIST OF FIGURES

## NOMENCLATURE

| | |
|---|---|
| FTIR | - Fourier Transform Infrared Spectrophotometry |
| UV | - Ultra-Violet Spectroscopy |
| AC | - Activated carbon |
| TGA | - Thermo-Gravimetric Analysis |
| SEM | - Scanning Electron Microscopy |
| TDS | - Total dry solids |
| XRD | - X-ray Diffraction |
| HPLC | - High Pressure Liquid Chromatography |
| TMP | - Transmembrane Pressure |
| kDa | - kilo Dalton |
| kPa | - kilo Pascal |
| g/L | - gram per litre |
| MF | - Microfiltration |
| NF | - Nanofiltration |
| UF | - Ultrafiltration |
| RO | - Reverse Osmosis |

# CHAPTER 1

# INTRODUCTION

## 1.1 BACKGROUND AND MOTIVATION

Biorefining has been defined as the sustainable conversion of biomass into a variety of valuable products and energy. By-products of the forestry industry are attractive raw materials for biorefineries because they do not require land that could otherwise be used for agricultural purposes. The forest biorefinery has the potential to generate additional products and increase profit margins for the pulp and paper industry (Moshkelani *et al*, 2012). Due to the decline in the reserves of natural resources and environmental concerns, recent and current research is focused on investigating ways of converting biomass/waste into marketable products and energy (Nzihou, 2010).

The forest biorefinery has received much attention from the pulp and paper sector in industrially mature countries primarily in North America and Western Europe as a potential way to diversify its product mix and generate new revenue streams. This has driven traditional manufacturing countries like Canada to take a fresh look at their renewable resources and seek alternatives to convert into sustained and profitable businesses (Moshkelani *et al*, 2012; Marinova *et al*, 2009). The implementation of biorefinery units in existing pulping mills is an attractive option especially when the forest industry is going through a period of continuing economic uncertainty as it is presently the case and closures of inefficient mills that have devastating social and economic consequences on small towns dependent on this industry for their livelihood (Moshkelani *et al*, 2012).

Lignin, a by-product of chemical pulping, is the most abundant source of aromatic compounds in nature and can generate a large amount of chemical reagents or adhesives to replace those derived from oil, and it could replace some or all of the fossil fuel currently used in the lime kiln at a Kraft mill (Pandey and Kim, 2011). It can be used as a biofuel, binder, dispersant or emulsifier, in phenolic resins, as precursor for carbon fibres, as a wet strength additive to Kraft liner, as a flocculating agent after chemical modification, and in road additives (Jönsson *et al*, 2008; Moshkelani *et al*., 2012; Wallberg and Jönsson, 2006). Additionally, it is a feasible raw material for many valuable substances such as activated carbon, vanillin, vanillic acid, ion-exchange agents, artificial fertilizers and complexing agents (Dafinov *et al*., 2005). An example is phenol-formaldehyde resins, in which part of phenol can be replaced with lignin. Its diversity of functional groups allows it to be used as a chelating agent for removing heavy metals from industrial effluents (Toledano *et al.*, 2010).

The common techniques for extracting lignin from black liquor are precipitation and membrane filtration (Dafinov *et al*., 2005; Wallberg *et al*., 2005). The extraction method employed should effectively separate the lignin from the black liquor, without causing an imbalance of the cooking chemicals, $Na_2S$ and NaOH. Drawbacks of using precipitation include the use of $H_2SO_4$ which upsets the liquor cycle chemical balance with excess sulphur and the process of filtering and separating the lignin precipitate is hampered by the formation of colloids (Toledano *et al*., 2010). Consequently, lignin separation by membrane processes has been advocated for to avoid these problems. The qualities that make membrane processes the ideal technique for separation purposes in biorefineries include their excellent fractionation capability, comparatively low energy requirement and minimal chemical consumption (Banerjee and De, 2012; Jönsson and Wallberg, 2009).

Factors that influence the performance of membrane filtration processes include, amongst others, membrane material, membrane pore size and the module geometry as well as the feed concentration, feed velocity and the transmembrane pressure drop (Mondor *et.al.*, 2000). Membrane modules, which are the housing for the membrane set up, are available in several geometries including plate and frame, spiral wound, tubular and hollow fibre modules (Banerjee and De, 2012). The rectangular geometry is used for spiral wound modules and for tubular and hollow fibre modules cylindrical geometries are used. Another module that is convenient and extensively utilized for laboratory scale experiments is the stirred cell (Sarkar, 2013). Experiments in a stirred cell can be conducted to validate any concept of separation or performance of membranes for a particular application (Banerjee and De, 2012).

Several studies have been undertaken to investigate the extraction of lignin from black liquor using ultrafiltration (Bhattacharjee and Bhattacharya, 1993; Satyanarayana *et.al*, 2000; Wallberg *et al*., 2003; Dafinov *et al*., 2005; Bhattacharje and Bhattacharya, 2005; Wallberg and Jönsson, 2006; Wallberg *et al*., 2006; Jönsson *et al*., 2008; Toledano *et al*., 2010). Ultrafiltration experiments were carried out by De and Bhattacharya (1996) in a rectangular cross flow ultrafiltration cell using low and high rejecting membranes in order to predict the flux of Kraft black liquor. The dependence of steady state flux and rejection on operating conditions such as pressure difference, cross flow velocity and feed concentration was investigated during the experiments. These results were used in the development of a model used to predict flux and real rejection for osmotic pressure controlled ultrafiltration. The model predictive results were compared to experimental results and only the results obtained by using low rejection membranes showed excellent agreement without the observation of any discrepancies. A stirred cell, modified to operate on a continuous mode was used by Bhattacharjee *et.al,* (2006) to carry

out ultrafiltration of black liquor. Experiments were conducted to investigate the variations of solute permeability and reflection coefficient with process variables such as bulk concentration, pressure difference and stirrer speed. Variations of these parameters with process variables were used to develop a dynamic model capable of predicting permeate flux and rejection at any time and the simulation results showed good agreement with the experimental results.

## 1.2 PROBLEM STATEMENT

### 1.2.1 Underutilization of lignin

Lignin is an amorphous and highly branched polymer of phenylpropane units, which can account for up to 40% of the dry biomass weight. Its structure suggests that it can serve as a precursor of valuable chemicals if it could be fragmented into smaller units. It is the main energy carrier in chemical pulp mills and its heat value is commonly recovered in recovery boilers by means of incinerating the black liquor which contains cooking chemicals, lignin derivatives and low molecular weight organics. The pulp and paper industry produces 40-50 million tons of lignin per year and only 1.5% is commercialized as lignosulphonates or Kraft process derived lignin. Thus it remains relatively underutilized to its potential.

### 1.2.2 Production bottlenecks in mills

Many existing Kraft mills are operating at or above their design capacity and the removal of some of the lignin from Kraft black liquor can allow increased pulp production. Pulp production is often limited by the amount of black liquor that can be incinerated in the recovery boiler and removal of some of the lignin can decrease the amount of black liquor solids per tonne of pulp as

well as the heating value of the solids. This would allow an increase in pulp production for a given load on the recovery boiler. A lignin extraction process could at the same time remove certain non-process elements such as silica and aluminium from the black liquor.

## 1.3 AIM AND OBJECTIVES

### 1.3.1 Aim

The main focus of this research was to study the extraction of lignin from Kraft black liquors by ultrafiltration using polymeric membranes in a batch stirred cell.

### 1.3.2 Specific Objectives

The following activities were carried out to meet the objectives of the study:

#### 1.3.2.1 Characterization of black liquors generated in South African mills.

The black liquor was characterized for lignin concentration, hemicelluloses content, solids concentration and ash content.

#### 1.3.2.2 Ultrafiltration study

- Determination of the hydraulic resistance of each membrane was investigated
- Investigation of the effect of different cut-off sizes of membranes on the permeate flux and retention of lignin from black liquor

- Investigation of the effect of transmembrane pressure on the permeate flux and retention of lignin
- Investigation of the effect of stirring rate inside the stirred cell on the permeate flux and retention of lignin
- Investigation of the effect of feed concentration on the permeate flux and retention of lignin

1.3.2.3 Modelling

- To develop models to predict the permeate flux at different experimental conditions of pressure, concentration and stirring rate

# CHAPTER 2

# LITERATURE REVIEW

## 2.1 INTRODUCTION

This chapter discusses previous investigations conducted by several researchers where ultrafiltration was used to extract lignin from black liquors using different membranes and setups. The chapter starts off with a discussion on lignin (its properties, extraction from lignocellulosic materials, isolation from black liquor as well as its application). This is followed by a discussion on the biorefinery concept as well as its potential integration into existing pulping mills such as the Kraft process. The Kraft pulping process as well as the properties and composition of black liquor are also discussed. A discussion on membrane technology is also presented and a thorough discussion on the concept of fouling is also included. One way to valorize lignin is by its conversion into a high-value product such as activated carbon, therefore this chapter is concluded by discussing previous investigations undertaken to convert lignin into activated carbon with an intention of using it as an adsorbent.

## 2.2 LIGNIN

Lignin is one of the main constituents of lignocellulosic biomass, along with cellulose and hemicelluloses. It is a cross-linked macromolecular material based on a phenylpropanoid monomer structure (Doherty *et al.*, 2011; Toledano *et al.*, 2010). The cellulose microfibrils

(formed by ordered polymer chains that contain tightly packed, crystalline regions) are embedded within a matrix of hemicellulose and lignin as shown in Figure 2.1. Covalent bonds between lignin and the carbohydrates have been suggested to consist of benzyl esters, benzyl ethers and phenyl glycosides (Doherty *et al.*, 2011). In its natural state, or as found in plants, it is referred to as protolignin.

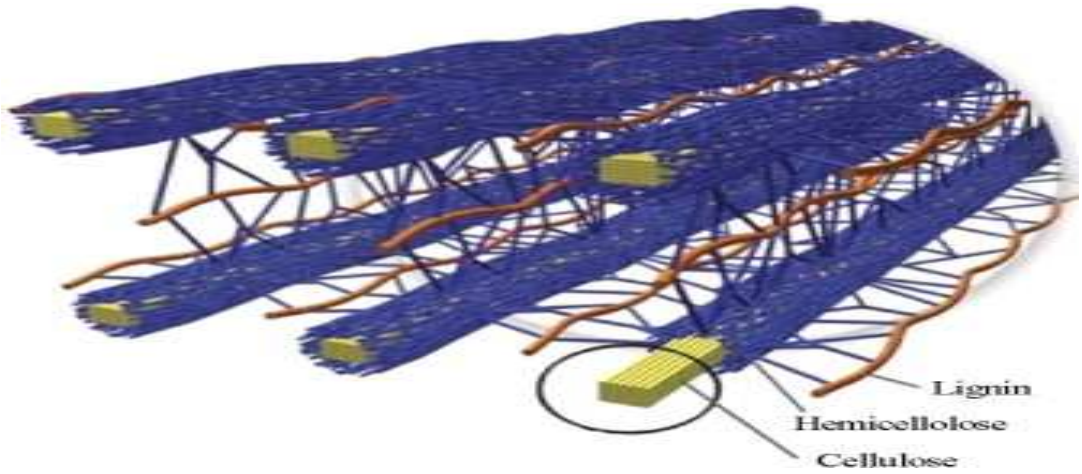


Figure 2.1 Cellulose strands surrounded by hemicellulose and lignin (Doherty *et al*., 2011)

Lignin is primarily a structural material to add strength and rigidity to cell walls and constitutes between 15 wt% and 40 wt% of the dry matter of woody plants. It is more resistant to most forms of biological attack than cellulose and other structural polysaccharides and plants with higher lignin content have been reported to be more resistant to direct sunlight and frost. In vitro, lignin and lignin extracts have been shown to have antimicrobial and antifungal activity, act as antioxidants, absorb UV radiation, and exhibit flame-retardant properties (Doherty *et al.*, 2011).

According to Buranov and Mazza (2008) the estimated amount of lignin on earth is 300 billion metric tonnes with an annual biosynthetic production rate of 20 billion metric tonnes. Thus, lignin is expected to play an important role as raw material for the world's bio-based economy for the production of bio-products and bio-fuels. The extraction of lignin from herbaceous plants is of paramount importance and the utilization of extracted lignin will lead to the industrial production of valuable food and industrial products such as vanillin, ferulic acid, vinyl guaiacol and optically active lignans, the dimers of monolignols.

The composition of lignin varies mainly in function of their origin (softwoods, hardwoods or herbaceous crops) but also of several factors such as growth conditions, harvesting and drying of the lignocellulosic biomass and the treatment employed during its transformation (Toledano *et al.*, 2010). Its complex three-dimensional polymeric structure results from the condensation of phenylpropane units, where p-hydroxyphenyl alcohol (H), guaiacyl alcohol (G) and syringyl alcohol (S) are the main precursors. The monomer structures in lignin consist of the same phenyl-propenoid skeleton, but differ in the degree of oxygen substitution on the phenyl ring. The H-structure (4-hydroxy phenyl) has a single hydroxy or methoxy group, the G-structure (guaiacyl) has two such groups, and the S-structure (syringyl) has three (Doherty *et al*., 2011). The monomer structures are shown in Figure 2.2.

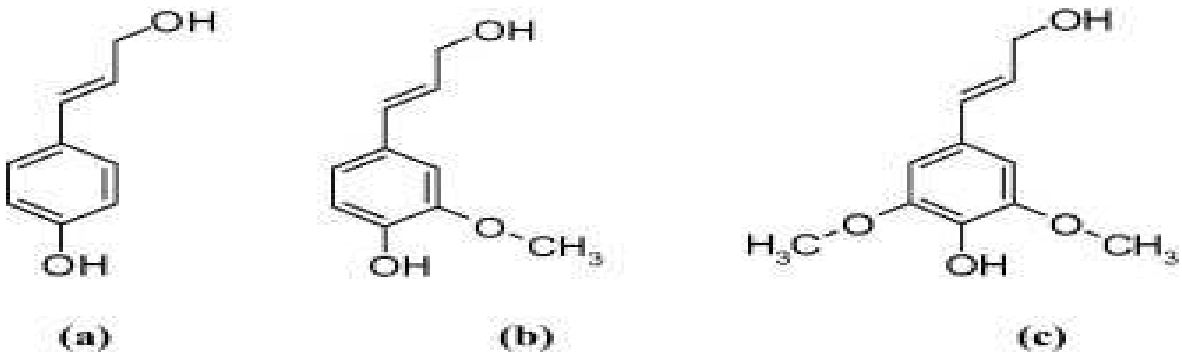


Figure 2.2 Monolignol monomer species: (a) p-Coumaryl alcohol (4-hydroxyl phenyl, H); (b) coniferyl alcohol (guaiacyl, G); (c) sinapyl alcohol (syringyl, S) (Doherty *et al*., 2011)

The exact structure of protolignin remains virtually unknown but improvements in methods for identifying degradation products and advancements in spectroscopic methods have elucidated many of the structural features of lignin (Chakar and Ragauskas, 2004). A generalized structure of lignin is shown in Figure 2.3.

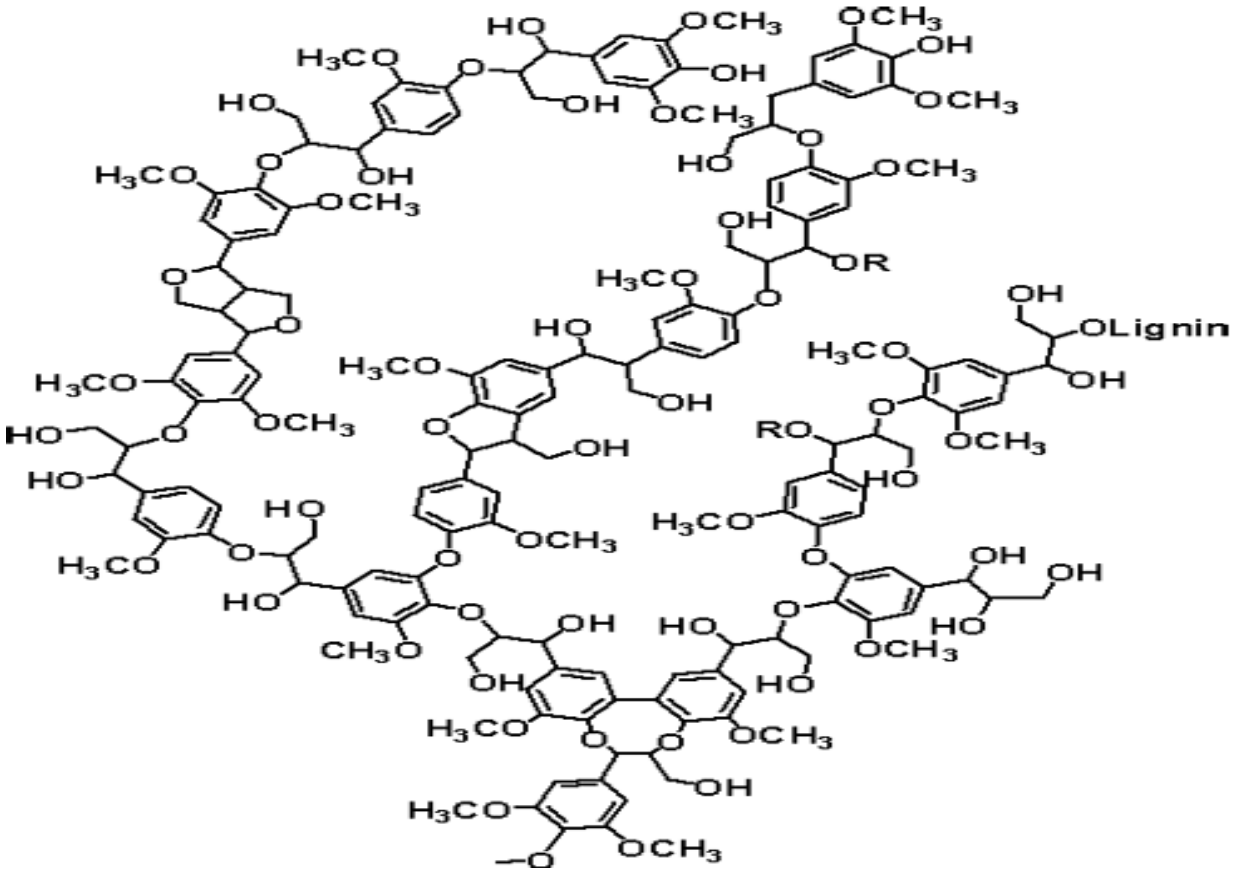


Figure 2.3 A generalized structure of lignin (http://www.lignoworks.ca/) Date accessed: 28 May 2015

Lignins may be divided into three broad classes, namely softwood, hardwood and grass lignin, according to their composition in structural units. A typical softwood lignin, also called guaiacyl or coniferous lignin, is made up of coniferyl alcohol units. Softwood lignins isolated by different methods and from different species are very similar in their structure. Hardwood or dicotyledonous angiosperm lignin is made up of coniferyl and synapyl alcohol units. The grass of monocotyledonous angiosperm lignin is made up of coniferyl, sinapyl and p-coumaryl units (Suhas *et al*., 2007).

The biosynthesis of lignin stems from the polymerization of the phenylpropane units. The polymerization process is initiated by the oxidation of the monolignol phenolic hydroxyl groups. The oxidation itself has been shown to be catalyzed via an enzymatic route. The enzymatic dehydrogenation is initiated by an electron transfer that yields reactive monolignol species with free radicals (see Figure 2.4), which can couple with each other. Subsequent nucleophilic attack by water, alcohols, or phenolic hydroxyl groups on the benzyl carbon of the quinone methide intermediate will restore the aromaticity of the benzene ring. The generated dilignols will then undergo further polymerization (Chakar and Ragauskas, 2004).Typical molecular masses of isolated lignin are in the range 1000-20000 g/mol, but the degree of polymerization in nature is difficult to measure, since lignin is invariably fragmented during extraction and consists of several types of substructures which repeat in an apparently haphazard manner (Doherty *et al.*, 2011).

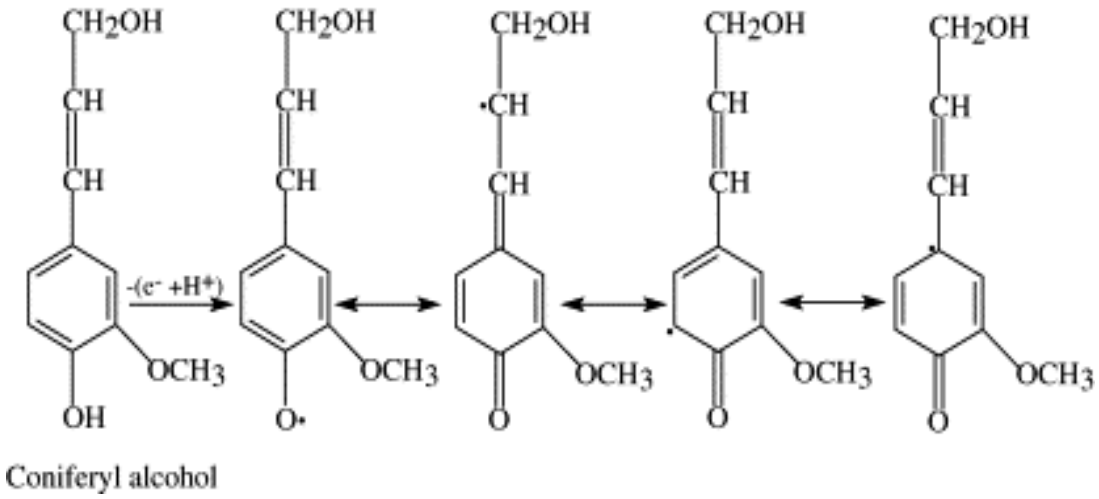


Figure 2.4 Dehydrogenation of coniferyl alcohol and the mesomeric radicals (Chakar and Ragauskas, 2004)

Both carbon-carbon and carbon-oxygen bonds between monomers are found in lignin and the most dominant functionality, accounting for about half the bonds between monomers in lignin from most sources, is a carbon-oxygen link between a p-hydroxy moiety and the β-end of the propenyl group (β-O-4) (Doherty *et al.*, 2011; Chakar and Ragauskas, 2004). Dibenzodioxocin, a linkage in softwood lignin, is estimated to account for a large component of the native bephenyl units in softwood lignin. Table 2.1 below shows the percent of linkages in lignin.

Table 2.1: Proportions of different types of linkages in lignin

| Linkage Type | Dimer Structure | Percent of Total Linkages (%) |
|---|---|---|
| β-O-4 | Phenylpropane β-aryl ether | 45-85 |
| 5-5 | Biphenyl and Dibenzodioxocin | 4-25 |
| β-5 | Phenylcoumaran | 9-12 |
| β-1 | 1,2-Diaryl propane | 7-10 |
| α-O-4 | Phenylpropane α-aryl ether | 6-8 |
| 4-O-5 | Diaryl ether | 4-8 |
| β-β | β-β-linked structures | 3 |

The fragmentation of the lignin macromolecule proceeds through the cleavage of the linkages holding the phenylpropane units together, with a concomitant generation of free phenolic hydroxyl groups. The presence of these hydroxyl groups increases the hydrophilicity of the lignin and the lignin fragments. As a result, the solubility of the lignin in the cooking liquor is increased. The carbon-carbon linkages, being more stable, tend to survive the pulping process

(Chakar and Ragauskas, 2004). During the initial delignification stage in alkaline pulping, phenolic α-O-4 linkages in lignin are cleaved and some phenolic β-O-4 linkages are cleaved, followed by the diffusion of extractable lignin components. The dominating reaction during the bulk stage is the cleavage of non-phenolic β-O-4 linkages. The final delignification stage has been assigned to the removal of residual lignin fractions, either by cleavage of carbon-carbon linkages or by carbohydrate degradation, releasing lignin-carbohydrate fragments (Sun and Tomkinson, 2001).

Lignin is a natural amorphous cross-linked resin that has an aromatic three-dimensional polymer structure containing a number of functional groups such as phenolic, hydroxyl, carbonyl, benzyl alcohol, methoxyl, and aldehyde groups (Guo *et al*., 2008). Different wood species have a variation in the distribution of functional groups and only approximate values are listed in Table 2.2.

Table 2.2 Functional groups in softwood and hardwood lignins (per 100 C-9 units) (Stenius, 2000)

| Functional group | Softwood lignin | Hardwood lignin |
|---|---|---|
| Phenolic hydroxyl | 20-30 | 10-20 |
| Aliphatic hydroxyl | 115-120 | 110-115 |
| Methoxyl | 90-95 | 140-160 |
| Carbonyl | 20 | 15 |

### 2.2.1 Lignin extraction from lignocellulosic materials

The extraction of lignin from lignocellulosic materials is conducted under conditions where lignin is progressively broken down to lower molecular weight fragments, resulting in changes to its physicochemical properties. Isolation of lignin from lignocellulosic materials is generally difficult due to condensation and oxidation reactions which occur during the isolation process (Suhas *et al.*, 2007). The source and method of extraction will have a significant influence on composition and properties of lignin. The majority of extraction and delignification processes occur by either acid or base-catalyzed mechanisms. Processes that are used to extract lignin from lignocellulosic materials include sulphide, Kraft, soda and other fractionation processes. The sulphite process involves the reaction of a metal sulphite and sulphur dioxide. The application of ionic liquids has been recently developed to fractionate lignocellulosic materials. Ionic liquids usually consist of a large asymmetric organic cation and a small anion and typically have negligible vapour pressure, very low flammability and a wide liquidus temperature range (Doherty *et al.*, 2011).

The main reactions that take place during the pulping process are: (a) the reaction between lignin and free sulphurous acid to form lignosulphonic acid, (b) the formation of the relatively soluble lignosulphonates with the cations, $Mg^{2+}$, $Na^{+}$, or $NH^{4+}$, and (c) the fragmentation of the lignosulphonates. The pulping reactions are usually conducted between 140$^{o}$C and 160$^{o}$C and the pH of the acid sulphite process is between 1.5 and 2.0, while the bisulphite process is between pH 4.0 and 5.0. The soda pulping process involves heating the biomass in a pressurized reactor in the temperature range 140-170$^{o}$C in the presence of 13-16 wt% alkali (typically sodium

hydroxide). Lignin recovered through extraction with sodium hydroxide is normally referred to as ‘soda lignin’ (Doherty *et al.,* 2011).

The Kraft process is the dominating pulping process by which wood chips are converted into pulp, the intermediate material from which a very broad spectrum of finished or semi-finished paper products are made (Marinova *et al.,* 2009). In the Kraft process wood chips are cooked in a digester where lignin and hemicelluloses are degraded into fragments and dissolved in the strongly basic delignification liquor. This delignification liquor is a mixture of sodium hydroxide and sodium sulphide and is referred to as white liquor. Delignification in the Kraft cook proceeds in three distinct phases: the initial phase, the bulk phase and the final or residual phase. The initial phase of delignification takes place up to a temperature of about 150$^{o}$C and is controlled by diffusion. The bulk phase includes the heating period from about 150-170$^{o}$C and the cooking treatment at 170$^{o}$C. The rate of delignification in the bulk phase is controlled by chemical reactions.

The final phase begins when about 90% of the lignin has been removed and marks the end of the cook. The remaining or residual lignin, typically 4-5 wt% is removed via bleaching techniques (Chakar and Ragauskas, 2004). The discharge from the delignification stage consists of cellulose fibre in suspension in the residual digestion liquor. The fibres are cleaned and separated from liquor in a series of washers and bleached to remove the residual traces of lignin and other impurities. Bleached pulp is then dried with steam and hot air. To recover the active cooking chemicals, the residual black liquor is concentrated in evaporators and burned in a recovery boiler to generate process steam and yield an inorganic smelt. The smelt is dissolved, recausticised by live lime produced on site and returned to the digester as white liquor (Moshkelani *et al.,* 2012). A simplified flow chart of the Kraft process is illustrated in Figure 2.5.

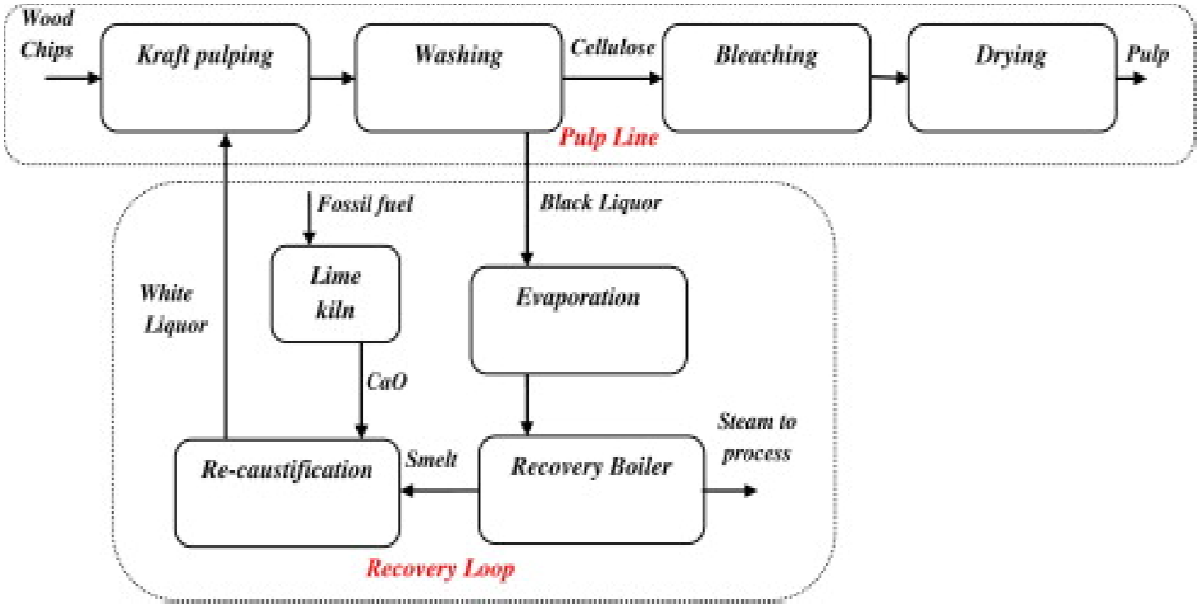


Figure 2.5: Simplified flow chart of the Kraft process (Moshkelani *et al*., 2012)

The reactions that occur during Kraft pulping are classified as degradation and condensation reactions. Degradation reactions lead to the liberation of lignin fragments and also enhance their dissolution whereas condensation reactions lead to the formation of alkali-stable linkages and are therefore undesirable. The prevalent degradation reactions during Kraft pulping are the cleavage of the α-aryl and β-aryl ether bonds and the reactivity of such linkages is sensitive to the type of phenolic group (free or etherified) present at the para position relative to the propane side chain. α-Aryl ether linkages in phenolic units are readily cleaved by the conversion of the phenolate unit into the corresponding quinine methide intermediate. For the condensation reactions, the hydrogen sulphide and sodium hydroxide anions have to compete with the lignin nucleophiles for quinine methide intermediates. The addition of the nucleophile to the quinine methide is reversible, and the result of this competition will not only depend on the nucleophilicity of the

species, but also on the ability of the addition product to undergo a fast, irreversible reaction (Chakar and Ragauskas, 2004).

### 2.2.2 Isolation of Kraft lignin from black liquor

The extraction of lignin from black liquor can be achieved by means of acid precipitation, ultrafiltration and by the application of selective solvents. Acid precipitation is the most commonly used method and it has reached the most advanced state of development and implementation (Moshkelani *et al*., 2012; Toledano *et al*., 2010). The optimal dry substance for precipitation is 27-30 wt% and the Kraft black liquor used for precipitation is commonly withdrawn after the third evaporation stage in the recovery system (Wallberg *et al.*, 2005). The acidification agents include carbon dioxide, sulphuric acid and waste acid from chlorine dioxide generation (Jönsson *et al.,* 2008). The pH of the black liquor is lowered using carbon dioxide and after filtering the lignin cake is washed in acidic conditions (pH 4) with sulphuric acid and the wash filtrates are returned to the evaporation section of the Kraft process (Moshkelani *et al.*, 2012). The disadvantage of this method is the formation of colloids which can complicate the process of filtration and separation, resulting in low purity of the lignin obtained (Toledano *et al.*, 2010).

The application of selective solvents such as ionic liquids allows obtaining lignin structures of low molecular weight, used in the synthesis of high added value products, but with very high production costs. Ultrafiltration is a promising way of separating lignin from Kraft black liquors. It enables obtaining lignin fractions with defined molecular weight distributions without the

consumption of chemicals. High value chemicals have to be recovered and returned to the process when lignin is extracted from the black liquor and the separation of lignin and cooking chemicals is achieved by concentrating the liquor. Ultrafiltration has the ability to separate high-molecular-weight lignin from low-molecular-weight cooking chemicals. Lignin is retained and the cooking chemicals pass through the membrane during the concentration process (Wallberg *et al.*, 2003).

### 2.2.3 Application of lignin

As a highly cross-linked material with widely varying functionality, lignin may not readily be characterized to give meaningful molecular weight data, but other parameters more directly relevant to end-use properties may be assessed. The reactivity and physicochemical properties of lignins are dependent to a certain extent, on their molecular weight distribution. Here are a number of physicochemical properties which suggest a bright future for lignin-based products (Doherty *et al.*, 2011):

- Compatibility with a wide range of industrial products
- Presence of aromatic rings providing stability, good mechanical properties, and the possibility of a broad range of chemical transformations
- Presence of other reactive functional groups allowing facile preparation of graft copolymers
- Good rheological and visco-elastic properties for a structural material
- Good film-forming ability
- Small particle size
- Hydrophilic or hydrophobic character depending on origin, allowing a wide range of blends to be formed

The compatibility of lignin with different polymer types has been examined extensively because it possesses easily-functionalisable hydroxyl and carboxylic acid groups. In principle, lignin can form composite materials with natural or synthetic polymers because its hydrophilicity can be controlled. The physicochemical qualities of lignin listed above indicate that in many cases it can improve the tensile strength and bulk modulus of these biopolymers and protect the composite against oxidative degradation under UV light or elevated temperature. Lignin can be blended with natural or synthetic polymers to form, amongst others, the following blends; protein-lignin blends, starch-lignin blends, polyhydroxyalkanoates, polyactides and polyglycolides, epoxy resin blends, phenol-formaldehyde resins, lignin-polyolefin blends, lignin-vinyl polymer blends, lignin-polyester blends, lignin-containing polyurethanes and lignin-polyurethane blends, rubber-lignin blends and lignin-graft-copolymers (Doherty *et al.*, 2011).

## 2.3 BIOREFINERY

Biorefining has been defined by the International Energy Agency as the sustainable processing of biomass into a spectrum of marketable products and energy (Moshkelani *et al.*, 2012). The integration of biorefinery units into existing pulping mill like the Kraft process can provide opportunities for diversifying the industry product mix and penetrating new profitable markets which can generate substantial revenues and profits. This concept has considerable economic advantages over autonomous grassroots biorefineries due to the availability of installed infrastructures, supplier and services networks, direct access to feedstocks, and skilled labour force (Moshkelani *et al.*, 2012).

Biomass resources include primary, secondary and tertiary sources. Primary resources are produced directly by photosynthesis and are taken directly from the land. They include perennial short-rotation woody crops and herbaceous crops, the seeds of oil crops, and residues resulting from the harvesting of agricultural crops and forest trees. Secondary resources result from the processing of primary biomass resources physically, chemically or biologically. Tertiary resources are post-consumer residue steams including animal fats and greases, used vegetable oils, packaging wastes and construction and demolition debris (Nzihou, 2010).

Conversion processes for biomass are often referred to as first or second generation processes, depending on the raw materials used. The majority of currently operating plants belong to the first generation and produce mostly bio-fuels like bio-ethanol and bio-diesel from sugar or starch containing plants and oil seeds. The so-called second generation biorefineries use the organic waste fraction from agriculture and lignocellulose provided in the form of straw or maize stover, wood harvest residues and fast growing wood and waste timber. These raw materials are inexpensive, available in great quantities and have lower impact on food production and prices. The quality of bio-fuels produced from these materials is higher than that of the common fossil fuels and they can substitute them at any dilution ratio (0-100%) without any need for alterations to the fuel consuming engines or only minor changes (Nzihou, 2010).

In most cases, lignocellulose feedstocks are currently reserved for thermo-chemical conversion because the additives (enzymes) and techniques for the hydrolysis of cellulose to obtain starch or sugar are still in their infancy. Thermo-chemical processes include the production of bio-crude oil by pyrolysis or hydrothermal treatment or gasification to produce synthesis gas. Subsequently

conventional processes like Fischer–Tropsch synthesis or other catalytic routes lead to bio-fuels and basic chemicals like methane, methanol, ethanol (Lyko *et al*., 2009).

The biorefinery model is similar to that of the petroleum refinery, but in contrast to the petroleum refinery, the biorefinery uses renewable resources. The biorefinery is based on two-platform concept; the biochemical platform and the thermo-chemical platform. The biochemical platform deals with the biological and chemical conversion of sugars derived from the carbohydrate fraction of the biomass in order to produce precursor molecules that could be converted into a number of high-value chemicals or materials. In the thermo-chemical platform, biomass is transformed into gaseous or liquid intermediate chemicals that can be upgraded to heat, power, transportation fuels or commodity chemicals (Marinova *et al.*, 2009).

The integration of biorefinery technologies into the receptor Kraft should be done in a sustainable manner in order to minimize the environmental impact. This is achieved by reducing greenhouse gas emissions of the total integrated site. The biorefinery options that can be integrated in the Kraft process include (Marinova et al., 2009; Moshkelani *et al.,* 2012):

- Hemicelluloses extraction from wood chips prior to pulping. Hemicelluloses and the majority of the lignin are captured in the black liquor and burnt in the recovery boiler to produce steam. Because the heating value of hemicelluloses is only half that of lignin, removing them from wood chips prior to pulping will provide Kraft pulp mills with the opportunity to produce value added products such as polymers, fuels and chemicals. Other benefits include increased delignification rate, decreased alkali consumption and reduced organic and inorganic load to the recovery cycle resulting in increased pulp production.

- Lignin recovery from black liquor. Its structure suggests it could play a role as a chemical feedstock, particularly in the formation of supramolecular materials and aromatic chemicals. An immediate option is to use lignin within the pulp mill for heat and power generation
- The wood residues can be gasified to produce synthetic gas that can be used as a source of heat, power, fuels and chemicals. Synthetic gas is a gas mixture composed of carbon monoxide, carbon dioxide and hydrogen (Nzihou, 2010).

The advantage of removing lignin from the black liquor is to reduce the load on the recovery boiler which is the bottleneck for pulp production. A lignin extraction process may also serve as a kidney to remove certain non-process components, such as silica and aluminium (Jönsson and Wallberg, 2009). The evaporator capacity can also be increased by extracting the lignin because the viscosity of lignin-depleted black liquor is lowered and can therefore be evaporated to a higher content of dry substances (Wallberg and Jönsson, 2006). Lignin extraction is possible through acid precipitation, electrolysis and ultrafiltration. The integration of lignin extraction stage in the Kraft process has an effect on energy demand. This is because the extraction of lignin from the black liquor decreases the steam production capacity of the reference mill recovery boiler. This deficit in steam is partially compensated by increasing the feed rate of wood chips to the Kraft process (Moshkelani *et al.,* 2012).

## 2.4 BLACK LIQUOR

Black liquor is generated from the pulping process when the wood components are dissolved in alkaline cooking liquor. All the organic compounds are dissolved except cellulose which remains insoluble. About 50% of the wood is dissolved in the cooking liquor and the main organic constituents that are present in the black liquor include ligneous material (poly-aromatic), saccharinic acids (hydroxyl acids), formic and acetic acid, and extractives. These compounds make up about 30-45 wt%, 25-35 wt%, 10 wt% and 3-5 wt%, respectively. Black liquor also contains about 1% methanol and inorganic elements, mainly sodium (17-20 wt %) and sulphur (3-5 wt %). It is characterized by high alkalinity (4-20 g/L NaOH, pH 13-14), high dry substance content (15-20 wt %) and high temperature (140-170$^{o}$C) (Wallberg and Jönsson, 2006). The chemical oxygen demand varies from 10000 to 120000 mg$O_2$/L depending on the pulping process applied (Dafinov *et al.*, 2005). The black colour derives from lignin compounds coloured by alkali and dissolved to liquor.

Physical characterization of black liquor is carried out to evaluate its solids content, density, calorific heating value and viscosity. Chemical characterization is carried out to evaluate elemental composition, lignin (concentration and molar mass) and organic to inorganic ratio (Cardoso *et al.*, 2009). The total dry solids (TDS) content is determined by drying the weighed samples at 105$^{o}$C and determining the weight of the residue. The ash content is measured by heating the residue from the TDS measurement to 950$^{o}$C and weighing the sample afterwards. The ash content is indicative of the concentration of inorganic matter in the sample. Lignin contains phenolic groups that absorb UV radiation and its concentration is measured as the light absorption at a wavelength of 280 nm. The concentration of inorganic elements is determined by inductively coupled plasma atomic emission spectroscopy (Wallberg *et al.*, 2005).

The black liquor composition depends on the type of the raw material processed and the operational conditions of the pulping stage. The raw material could be softwood (such as pine), hardwood (such as eucalyptus) or fibrous plants (such as bamboo). The black liquor composition affects its properties, basically those that govern its behaviour in the recovery unit. The concentration, molar mass and molecular conformation of lignin and polysaccharide present in the black liquor strongly affect its rheological behaviour. Liquors with high lignin and polysaccharide concentrations tend to have a high viscosity. This is because these two compounds can cluster into amorphous and voluminous molecules of high molecular mass. Conversely, liquors with low lignin and polysaccharide concentrations tend to present a lower viscosity. This is because these compounds can agglomerate in a more compact and spherical molecular structure (Cardoso *et al.,* 2009).

The conventional treatment of black liquor is water evaporation until the dry matter reaches a concentration of 70-80 wt%. The residue is then incinerated and energy is produced, which can be used in the pulping process. A recovery of up to 80% of the digesting chemicals can be achieved from the resulting ash. A small part of the black liquor is used as a source of lignin that can be extracted either by precipitation or diafiltration (Dafinov *et al.,* 2005). The black liquor properties and the continuous operation of the industrial black liquor recovery plant can be affected by the presence of inert or non-processing elements (NPE) in the black liquors (potassium, chlorine, calcium, aluminium, silicon and iron ions). The surfaces of equipment walls are corroded by the incrustation of the non-processing elements on the walls, which causes operational problems. At low temperatures and solid concentrations, aluminium, calcium and silicon ions form, with the organic compounds, complexes that can avoid building up an insoluble crust on evaporator walls. At high liquor temperatures and solid concentrations, these

complexes, when formed, become destabilized, releasing calcium, aluminium, and silicon ions, which form calcium carbonate and/or aluminium silicate, incrusting on the wall-surfaces of heat exchange evaporators (Cardoso *et al.,* 2009).

## 2.5 MEMBRANE TECHNOLOGY

A membrane can be referred to as a phase that acts as a barrier to prevent mass movement but allows restricted and/or regulated passage of one or more species through it, thus, a membrane can be gaseous, liquid or solid or combinations of these. Membranes can be classified according to these criteria (Cheryan, 1986):

- Nature of the membrane (natural or synthetic)
- Structure of the membrane (porous or non-porous, its morphological characteristics, or as liquid membranes)
- Application of the membrane (gaseous phase separations, gas-liquid or liquid-liquid)
- Mechanism of membrane action (adsorptive or diffusive or inert membranes)

Membranes can also physically or chemically modify the permeating species, prevent permeation or regulate the rate of permeation. Depending on the membrane's ability to alter the chemical nature of the permeating species, it can be classified as passive or reactive.

Membrane separation processes can be classified as microfiltration (MF), ultrafiltration (UF), nanofiltration (NF) and reverse osmosis (RO). These methods differ in membrane type, operating

conditions required and their application fields. Table 2.3 lists the membrane separation processes (Toledano *et al*., 2010).

Table 2.3 Operating conditions and applications of different separation processes

| Process | Membrane type and pore size | Driving force (bar) | Applications |
|---|---|---|---|
| MF | Symmetric microporous (0.1-10µm) | 1-5 | Sterile filtration, clarification |
| UF | Assymetric microporous (1-10nm) | 1-10 | Separation of macromolecular solutions |
| NF | Thin-film membranes 0.001-0.01µm | 10-30 | Removal of hardness and desalting |
| RO | Asymmetric skin-type (0.5-1.5nm) | Up to 200 | Separation of salts and micro-solutes from solutions |

Membrane separation processes do not require that there should be a suitable density difference between the two phases that are to be separated. The application of hydraulic pressure to speed up the transport processes is what distinguishes MF, UF, NF and RO membrane processes. The nature of the membrane controls which component permeates and which component is retained. Ideally, reverse osmosis retains all components other than the solvent itself, while ultrafiltration retains only macromolecules or particles larger than about 0.001-0.02 µm. Microfiltration processes are designed to retain particles in the range 0.10-10 µm. particles larger than 10 µm are best handled by conventional filtration processes. Ultrafiltration can be considered as a method

for simultaneously purifying, concentrating, and fractionating macromolecules or fine colloidal suspensions. Reverse osmosis can be applied as a dewatering technique and microfiltration is used for separating suspended particles from dissolved substances in a feed stream (Cheryan, 1986).

UF and RO are continuous molecular separation processes that do not involve a phase change or interphase mass transfer. UF and RO processes involve pumping the feed solution under pressure over the surface of a suitably supported membrane, of the appropriate chemical nature and in the optimum physical configuration. In the UF process, the solvent and smaller species are forced through the pores of the membrane by the pressure gradient across the membrane while the larger molecules are retained. The retained phase will be enriched in the retained macromolecules while the permeate stream will be depleted of the macromolecules. The retentate will also contain some of the permeable solutes. It may be the same or higher concentration than in the permeate stream, depending on that component's rejection by the membrane (Cheryan, 1986).

Several polymers and other materials are used for the manufacture of permselective membranes. These membranes include cellulose acetate, polyamide, polysulphone, composite materials and mineral or ceramic membranes. Cellulose acetate is prepared from cellulose by acetylation (reaction with acetic anhydride, acetic acid and sulphuric acid). The major traditional source of cellulose is wood pulp or cotton linters, although there has been some recent interest in microcrystalline cellulose, which is chemically modified wood pulp. Polyamide membranes are characterized by having an amide bond in its structure. Polysulphone membranes are used

mainly for ultrafiltration applications due to the following characteristics: (a) wide temperature limit (b) wide pH tolerances (c) wide range of pore sizes available for ultrafiltration applications (Cheryan, 1986).

Composite membranes have been primarily developed for reverse osmosis applications. Composites have a thin dense polymer skin or barrier layer formed over a microporous support film. Asymmetric membranes are made in a one-step procedure, while composite materials are made by a two-step procedure. Ceramic membranes are formed by deposition of inorganic solutes on to microporous supports. Zirconium oxide is a commonly used solute, while porous carbon tubes and porous metal tubes are common. Since ceramic membranes are made of inorganic materials, they should have little or none of the disadvantages associated with polymeric membranes. Both membrane and support tube should possess a high degree of resistance to chemical and abrasion degradation and should tolerate a wide range of pH and temperature ranges (Cheryan, 1986).

Membrane technology equipment can be constructed in four basic designs: (a) Tubular, with inner diameters >10mm, (b) Hollow fibres, with inner diameters less than about 1.3mm, (c) Plate-type units, (d) Spiral-Wound modules. Laboratory scale apparatus used for ultrafiltration include dead-end cells, stirred cells and thin-channel cells. Dead-end cells are ideal for separating very dilute solution of macromolecules in small volumes. They are used widely for studying binding and interactions of ligands and minerals to proteins. Stirred cells are suitable for bench-top feasibility studies. Agitation is provided with a magnetic stirring bar placed as

close as possible to the membrane surface. Stirred cells are useful in evaluating the rejection properties of membranes under limited conditions. They are not recommended for evaluating the engineering parameters of a membrane process. In thin-channel cells, the retentate is pumped through narrow channels or slits on top of the membrane at high shear rates. The retentate is returned to the feed reservoir (Cheryan, 1986).

Membrane processes have been used in pulp and paper mills since the late 1960s and the majority of applications have been aimed at the treatment of bleach plant effluent and fractionation of spent sulphite liquor. The qualities that make membrane processes ideal separation processes in biorefineries include, amongst others, their excellent fractionation capability, low chemical consumption and low energy requirement. The main benefits of membrane processes in lignin extraction are the possibility of withdrawal of the liquor at any position, without adjustment of the pH or temperature, and the possibility to control the molecular mass of the lignin fraction by the membrane cut-off (Jönsson *et al.*, 2008). The size of the lignin molecules can vary between 1 kDa and 100 kDa within the same sample. The high structural diversity and high molecular weight distribution of lignin makes its use a difficult task and fractionation has become one of the best ways to obtain specific lignins (Toledano *et al.*, 2010). The following sections describe the investigations that have been undertaken to extract valuable components from process streams such as black liquor using various types of membranes and setups.

### 2.5.1 An overview of previous ultrafiltration experiments

Ultrafiltration of black liquor in a stirred batch cell using a cellulose acetate membrane of 5 kDa was carried out by Bhattacharjee and Bhattacharya (1993). The membrane parameters such as solute permeability and reflection coefficient were determined to characterise the membrane. The effects of operating variables such as pressure, flow condition and bulk concentration on limiting flux phenomena was studied and a correlation was developed to relate polarized layer resistance with concentration polarization modulus, osmotic to applied pressure ratio and Reynolds number. It was found that the flux for black liquor was comparatively lower that other solutes such as PEG which could be attributed to the increased thickness of the polarized layer. This is as a result of solutes in black liquor that may have very high molecular weight (10 kDa or more) which could deposit on the membrane surface leading to an increase in resistance.

A comparative study on the ultrafiltration of Kraft black liquor using different flow modules was carried out by Satyanarayana *et.al*, (2000). The different modules investigated included the radial cross flow, rectangular cross flow and stirred cell. Effects of operating conditions such as stirring rate, feed concentration and pressure difference on the rejection and flux decline were investigated in each module. It was noted that at higher pressure, deposition on the membrane surface occurred at a faster rate. Consequently, osmotic pressure of the solution at the surface increased which reduced the driving force of the solvent transport. Therefore, the permeate flux was found to increase with a slower rate at higher pressures. For higher feed concentrations, concentration polarization was more severe which was reflected in depressed flux values observed in the study. From the study it was observed that flux increased gradually for high

Reynolds number ($Re$). As $Re$ number increased (by stirring or cross flow velocity), forced convection of the solutes prevented them from being deposited on the membrane surface. This led to an enhancement in permeate flux. For the rectangular cell it was found that the mechanism of flux decline over time was purely osmotic pressure controlled and that for stirred and radial cell it was controlled by the developing deposited layer on the membrane surface. The authors concluded that the observed rejection and permeate flux were higher in the stirred cell in comparison with the radial and rectangular cells.

The analysis of flux decline during ultrafiltration of Kraft black liquor was conducted by De *et.al,* (1997) using a stirred cell modified to operate in a continuous mode. The flux decline was divided into short time and long time domains and the effect of operating parameters such as applied pressure, feed concentration and stirrer speed was investigated during the experiments. In the study it was observed that the membrane resistance increased over successive runs which could be attributed to irreversible fouling of the membrane which led to permanent loss of membrane permeability. It was concluded that the initial flux decline was osmotic pressure controlled and was found to be rapid and could be complete within a few seconds. Flux decline for the long time domain was attributed to the gradual growth of a polarized layer over the membrane surface and could be modelled using a two parameter model.

Bhattacharje and Bhattacharya (2006) studied the performance of ultrafiltration of black liquor by using a laboratory fabricated stirred and rotating disk batch ultrafiltration cell. The study was carried out as an attempt to minimize flux decline in order to obtain enhanced flux for the

treatment of black liquor obtained from sulphite pulping industries. An asymmetric cellulose triacetate membrane with a cut-off size of 5 kDa was used for experimentation. Correlations for reduction of concentration polarization observed as a function of membrane rotation with different operating variables, like transmembrane pressure (TMP), stirrer speed and membrane rotation speed were obtained. The rejection of solutes was also correlated with different operating parameters. A new model was also developed based on pore-plugging theory in order to assess the performance of ultrafiltration. The authors concluded that membrane rotating was more efficient in reducing concentration polarization compared to stirring action.

Wallberg and Jönsson (2006) studied the separation of lignin from Kraft cooking liquors by ultrafiltration (UF) in continuous mode at temperatures above 100$^{o}$C. They used two ceramic membranes with cut-offs of 5 and 15kDa to investigate the effects of trans-membrane pressure (TMP), cross-flow velocity and temperature on the retention of lignin. The liquors were taken directly from a continuous digester and fed directly to the pilot plant without cooling, pH adjustment or pre-filtration, except for a screen in the digester wall. The membranes were made of $Al_2O_3$-$TiO_2$ with an active layer of $ZrO_2$. TMP had a significant effect on flux in the pressure interval investigated. For temperatures above 100$^{o}$C cross-flow velocity had a negligible effect on flux. The flux was found to increase with temperature in the temperature range studied. The flux was higher for the 15kDa membrane but the retention was higher for the 5kDa membrane. When treating softwood liquor the retention on the 5kDa membrane was 30% and on the 15kDa membrane was 20%. When treating hardwood liquor the retention was only 10% for the 5kDa membrane.

The fractionation of lignin from black liquors by continuous UF and selective precipitation was studied by Toledano *et al*, (2010). They used ceramic membranes with cut-off sizes of 5, 10 and 15 kDa. The black liquor solution was filtered successively by increasing the membrane cut-off and the permeate collected. From the gel permeation chromatography results it was found that ultrafiltration yielded fractions with more differentiated weight-average molecular weight than selective precipitation. For UF there was a clear trend of the decrease of the weight-average molecular weight as the cut-off used to obtain the fractions was smaller. As a result the polydispersity also decreased with the pore size. All fractions obtained by selective precipitation presented low polydispersity. Both fractionation techniques produced fractions with low polydispersity which indicated a high fraction of low molecular weight in different fractions. It was concluded that UF is the better fractionation method because the lignin obtained was less contaminated with hemicelluloses.

Wallberg *et al,* (2003) studied the fractionation and concentration of Kraft black liquor lignin with ultrafiltration using polymeric membranes of different sizes. The cut-off sizes of the membranes were 4, 8 and 20 kDa and the inner diameter of all the membranes was 12,5 mm. In the first series of experiments the retention of three UF membranes with different cut-off sizes was studied and in the second series of experiments the performance of one membrane was studied during concentration and diafiltration of black liquor. The temperature was maintained at $60^{o}$C for all experiments. The flux increased with an increase in TMP for the 8 and 20 kDa membranes and levelled off at a TMP of about 400 kPa. The flux of the 4 kDa membrane increased linearly with TMP in the entire pressure interval studied. Cake formation was attributed to the non-linear relationship between the flux and TMP for the 8 and 20 kDa

membranes. Lignin concentration was further increased from 120 g/L to 135 g/L by means of diafiltration. The lignin retention was 80, 67 and 45% for the membranes with cut-offs of 4, 8 and 20 kDa, respectively.

The concentration and purification of lignin in hardwood Kraft black pulping liquor by ultrafiltration and nanofiltration (NF) was studied by Jönsson *et al,* (2008). Tubular, polymeric membranes with nominal cut-off sizes of 4-100 kDa were used to investigate the influence of membrane cut-off on the retention of lignin and hemicelluloses during ultrafiltration of softwood and hardwood cooking liquor. In addition, a ceramic membrane with a cut-off size of 15 kDa was used to study the effect of TMP and cross-flow velocity on ultrafiltration of evaporated hardwood black liquor. The ceramic membrane used in the study was made of $Al_2O_3$-$TiO_2$. The results from UF experiments using polymeric membranes showed higher retentions of hemicelluloses and lower retention of lignin in hardwood liquor than in softwood liquor. For ultrafiltration experiments using ceramic membranes, it was found that the cross-flow velocity had a significant influence on flux.

### 2.5.2 Fouling

Fouling is a deterrent for the implementation of pressure driven membrane processes. Fouling takes place when flux declines with time of operation when all operating parameters, such as pressure, flow rate, temperature and feed concentration are kept constant. During the processing of a solution, the flux is lower than pure water flux for the following reasons: (a) change in membrane properties (b) change in feed solution properties (c) concentration polarization and (d)

membrane fouling. Changes in membrane properties can take place when membranes undergo a creep or compaction phenomenon caused by high pressures used in the separation process. Chemical deterioration can occur if the pH, temperature and other environmental factors are incompatible with the particular membrane. As the feed stream's solids levels increase, its viscosity and density increase, which decreases the diffusivity and the flux. A localized increase in solute concentration at the membrane surface also lowers flux due to either an increased hydrodynamic resistance in the boundary layer or due to higher local osmotic pressure decreasing the driving force (Cheryan, 1986).

Models that exist to explain the flux decline concept include resistance-in-series model, gel-polarization model and osmotic pressure model. These are represented by Equations 2.1-2.3, respectively (Satyanarayana *et al.*, 2000; De *et al.,* 1997; Schwarze et al., 2010). The resistance-in-series model is used to predict flux decline that occurs in the long term and it is of significance to process engineers in industry for design purposes. The osmotic pressure model is used to account for flux decline that occurs within a few seconds of start-up of operation. The gel-polarization model is based on these assumptions (Nicolas *et al.,* 2000); (i) Convection-diffusion is responsible for mass transfer and only perpendicularly to the membrane, (ii) The concentration does not affect solute diffusion coefficient and (iii) The solute density does not change in the polarization layer.

$$J_p(t) = \frac{\Delta P - \Delta \pi}{\mu[R_m + R_{osm} + R_d(t)]} \qquad (2.1)$$

$$J_p(t) = k \ln\left(\frac{c_m - c_p}{c_b - c_p}\right) \qquad (2.2)$$

$$J_p(t) = \frac{\Delta P - \Delta \pi}{\mu R_m} \qquad (2.3)$$

Where $J_p(t)$ is the permeate flux at anytime, $\Delta P$ is the pressure difference, $\Delta \pi$ is the osmotic pressure difference and $\mu$ is the viscosity. $R_m$, $R_{osm}$ and $R_d(t)$ represent the membrane hydraulic, osmotic pressure and deposited layer resistances, respectively. $c_m$, $c_p$ and $c_b$ represent the solute concentration in the membrane surface interface, permeate and bulk solutions, respectively.

The membrane resistance can be calculated from Equation 2.4:

$$R_m = \frac{\Delta P}{\mu J} \qquad (2.4)$$

The mass transfer coefficient k in Equation 2.2 can be evaluated from standard correlations and for a stirred cell the correlations are given as (De *et al.*, 1997):

$$Sh = \frac{kr}{D} = 0.285(Re)^{0.55}Sc^{0.33} \text{ for } Re < 32000 \qquad (2.5)$$

$$Sh = \frac{kr}{D} = 0.0443(Re)^{0.75}Sc^{0.33} \text{ for } Re > 32000 \qquad (2.6)$$

where r is the stirring radius and D is the diffusion coefficient.

Because the surface concentration at the membrane interface changes as ultrafiltration proceeds, physical properties like density and viscosity of the solution also change with time. To take into account the variations of these properties with the change in concentration in a stirred cell, the

Sherwood number correlation can be modified by introducing a correction factor $(Sc/Sc_m)^{0.22}$ to yield (De *et al.*, 2007):

$$Sh = \frac{kr}{D} = 0.285(Re)^{0.55}Sc^{0.33}(Sc/Sc_m)^{0.22} \qquad \text{for } Re < 32000 \qquad (2.7)$$

The impact of concentration polarization in dead end filtration systems such as stirred cells can be minimized by the imposition of a high shear field in the vicinity of the membrane surface. This is achieved by placing an agitator in close proximity to the membrane (Sarkar *et al.*, 2010). This results in the retardation of the increase in polarized layer resistance which finally reaches an asymptote leading to a steady state flux. Hydrodynamic conditions such as shear rates and convective mass transfer coefficients have an impact on ultrafiltration in stirred cells and the interfacial mass transfer and shear stresses are controlled by agitator rotational speed. These facilitate the back-mixing of rejected solute from the membrane interface and they vary with membrane configuration. In stirred cells, the flux uniformity is comparatively better and the influence of concentration polarization is reduced due to higher convective mass transfer rates in the system (Becht *et al.*, 2008).

The performance of an ultrafiltration unit is primarily affected by the operating Reynolds number. For a stirred cell, the Reynolds number is calculated as:

$$Re = \frac{\rho\omega r^2}{\mu} \qquad (2.8)$$

Where ω is the rotational velocity in radians/second and r is the stirrer outer radius

A high Reynolds number restricts the accumulation of deposited species on the surface of the membrane and facilitates the back mixing of solutes from the membrane interface to the bulk

solution. The enhancement of back-diffusion of solutes to the bulk solution results in the increase in permeate flux. Under these conditions the polarization resistance is approximately double the osmotic pressure resistance. The rate of back-diffusion of solutes from the membrane interface is retarded at low Reynolds number values because the influence of external forced convection is significantly reduced. The dominating resistances at low Reynolds numbers are the polarization and membrane hydraulic resistances and only a small extent of the total resistance is contributed by the osmotic pressure (Satyanarayana *et.al,* 2000).

In addition to the Reynolds number, the flow shear stress distribution on the membrane surface as a function of impeller rotational speed also has an impact on ultrafiltration in a stirred cell (Koutsou and Karabelas, 2012). To calculate the shear stress in a stirred cell, it is assumed that the stirrer resembles a flat blade impeller. The flow field is subdivided into an inner region and an outer region. The shear stress increases in the inner region up to the critical radius of the impeller where maximum shear stress in experienced, and decreases beyond the outer region. The critical radius of the impeller is given as (Becht *et al.,* 2008):

$$r_c = \frac{D_i}{2} 1.23 \left(0.57 + 0.35 \frac{D_i}{D_t}\right) \times \left(\frac{h}{D_t}\right)^{0.036} n_b^{0.116} \frac{Re_i}{1000+1.43Re_i} \qquad (2.9)$$

Where $D_t$ is the stirred cell diameter, h is the blade height, $n_b$ represents the number of stirrer blades and $Re_i$ is the impeller Reynolds number. The diameter used to calculate $Re_i$ is the impeller diameter and not the stirred cell diameter. The shear stress below and above the critical radius can be calculated as (Becht *et al.,* 2008):

$$\tau = 0.825 \mu \omega r \frac{1}{\delta} \quad \text{for } r < r_c \qquad (2.10)$$

$$\tau = 0.825\mu\omega r_c \left(\frac{r_c}{r}\right)^{0.6} \frac{1}{\delta} \quad \text{for } r > r_c \qquad (2.11)$$

The thickness of the momentary boundary layer ($\delta$) can be obtained from the relationship between the momentary boundary layer and the concentration boundary layer ($\delta_C$) which is given as (Becht et al., 2008) :

$$\frac{\delta}{\delta_C} = Sc^{0.33} \qquad (2.12)$$

The concentration boundary layer can be evaluated from the Landau-Lifshitz equation as (Becht *et al.*, 2008):

$$\delta_C = \frac{D_i}{Sc^{1/3}\sqrt{Re_r}} \qquad (2.13)$$

The momentary boundary layer ($\delta$) is obtained by combining Equations 2.12 and 2.13 to yield:

$$\delta = \sqrt{\frac{\mu}{\rho\omega}} \qquad (2.14)$$

The initial flux can be calculated based on Equation 2.15 as follows (Schwatze *et al.*, 2010):

$$J_0 = \frac{1}{A_m \rho_w}\left(\frac{\Delta m}{\Delta t}\right)_0 \qquad (2.15)$$

where $A_m$ and $\rho_w$ represent the membrane area and water density, respectively. The initial slope $(\Delta m/\Delta t)$ from the mass-time curves from which the permeate is less than 5-10% of the initial

feed volume is used to calculate the initial flux. The flux reduction, which is a measure of ultrafiltration performance, is calculated as follows (Schwatze *et al.*, 2010):

$$\mathrm{FR} = \left(1 - \frac{J_0}{J_w}\right) \times 100\% \qquad (2.16)$$

where $J_w$ is the pure water flux.

### 2.5.3 Blocking filtration laws for constant pressure filtration

Membrane blocking models are an alternate form of describing the decline in flux during the course of filtration (Iritani, 2013; Sarkar, 2013). As explained in the preceding section, the decline in flux may be as a result of pore blockage and/or the formation of a cake layer on the external membrane surface (Bowen *et al*, 1995). Foulants that are smaller than the membrane pores can deposit onto the pore walls and lead to pore constriction. On the other hand larger foulants have the potential of blocking the pore entrances, which could lead to a significant increase in resistance to filtration (Iritani, 2013). Among the mathematical expressions proposed to describe the fouling of the filter media due to pore blocking and cake formation during liquid filtration there is a series of laws referred to pore blocking laws that were originally proposed by Hermans and Bredée (1936). These laws included complete blocking, intermediate blocking, standard blocking and cake layer formation (Bowen et al., 1995). Numerous researchers (Hermia, 1982; Grace, 1956) made an effort to revise and reformulate the blocking laws in a common frame for constant pressure dead-end filtration of power-law non-Newtonian fluids (Sarkar, 2013; Iritani, 2013). For constant pressure filtration, the four blocking laws can be

expressed as a common differential Equation 2.17 with the two constants $k$ and $n$, which depend on the mode of filtration (Iritani, 2013):

$$\frac{d^2t}{dv^2} = k\left(\frac{dt}{dv}\right)^n \qquad (2.17)$$

where $v$ and $t$ are the filtrate volume per unit membrane area and filtration time, respectively. Equation 2.17 can be expressed in alternate form as (Iritani, 2013):

$$\frac{dJ}{dt} = -kJ^{3-n} \qquad (2.18)$$

where the blocking index n is a dimensionless filtration constant that characterizes the mode of the fouling model involved, with $n = 2$ for complete blocking, $n = 1.5$ for standard blocking, $n = 1$ for intermediate blocking and $n = 0$ for cake filtration. $k$ is the resistance coefficient which depends on the system, the filter medium, and the conditions of filtration (Iritani, 2013).

In the complete model is it assumed that each particle arriving to the membrane blocks some pores without superimposition of particles resulting in an attainment of medium permeability of the membrane with some open passage (Sarkar, 2013). For complete blocking Equation 2.18 can be rewritten as (Iritani, 2013):

$$J = J_o exp(-K_b t) \qquad (2.19)$$

where $K_b$ is the plugging constant of complete blocking law

For the standard blocking law it is assumed that the membrane consists of parallel pores of constant diameter and length, that the pore volume decreases proportionally to the filtrate volume passing through the membrane pores by particle deposit on the pore walls with eventual plugging of the pores and that the particles are in complete retention (Iritani, 2013). For standard blocking Equation 2.18 can be rewritten as (Bowen et al., 1995):

$$J = \frac{J_o}{\left(\frac{K_s J_o}{2} + 1\right)^2} \qquad (2.20)$$

where $K_s$ is the plugging constant of standard blocking law

With the intermediate blocking model it is assumed that foulants reaching the membrane directly block some membrane area or deposit on other already deposited fouling particles (Bowen et al., 1995). For intermediate blocking Equation 2.18 can be rewritten as (Iritani, 2013):

$$J = \frac{J_0}{k_i J_0 t + 1} \qquad (2.21)$$

where $k_i$ is the intermediate blocking constant

With the cake filtration mechanism it is assumed that flux declines after pore blockage due to formation and growth of cake layer on the membrane surface which offers resistance to the permeate flow. The resistance of the cake layer is thought to increase with the growth of the cake layer thickness which in turn leads to a gradual decline in permeate flux with time (Sarkar, 2013). For cake filtration Equation 2.18 can be rewritten as (Iritani, 2013):

$$J = \frac{J_o}{(1 + 2K_c J_o^2 t)^{1/2}} \qquad (2.22)$$

where $k_c$ is the plugging constant of cake filtration law

## 2.6 ACTIVATED CARBON AND ADSORPTION

Activated carbon is the collective name for a group of porous carbons manufactured by the treatment of a char with oxidizing gases or by carbonization of carbonaceous materials impregnated with dehydrating chemicals. All these carbons exhibit a high degree of porosity and an extended internal surface area. Activated carbons are the most important commercial adsorbents due to their good adsorption capacities towards a wide variety of pollutants. These pollutants include both organic and inorganic substances from the liquid or gaseous phases (Suhas *et al.,* 2007). Their high surface area, well-developed internal microporosity structure and the presence of a wide spectrum of surface functional groups allow them to be used in a wide variety of industrial applications. Adsorption with activated carbon is commonly used for the removal of toxic pollutants like heavy metals from industrial wastewater (Gonzalez-Serrano *et al.*, 2004; Yin *et al.*, 2007). Coals and lignocellulosic materials are commonly used as the raw material for activated carbon production (Hayashi *et al.,* 2000). These raw materials include wood, almond shells, olive stones, coconut shells, peach, apricot stones and apple pulp. The nature and structure of the raw material used for the preparation of activated carbon has an effect on its microporous properties (Cagnon *et al.,* 2009).

The demand for activated carbon is growing as environmental pollution is becoming a more serious problem but the drawback of using it as an adsorbent is its high cost (Guo *et al.*, 2008; Hayashi *et al.,* 2000). The use of carbonaceous residues and by-products from existing industrial processes as raw materials for the manufacturing of activated carbon has the potential to reduce costs through process integration (Montané *et al.,* 2005). Lignin is an ideal starting material for the production of carbon materials due to its high content of aromatic portions in the macromolecule and a molecular structure similar to bituminous coal (Kijima *et al.*, 2011; Suhas

*et al.,* 2007). It is available in high amounts at low cost. Lignin also contains a number of functional groups such as phenolic, hydroxyl, carboxyl, benzyl alcohol, methoxyl and aldehyde groups. These groups give lignin a potential to be used as an adsorbent material for removal of heavy metals from solutions (Guo *et al.,* 2008). A number of researches has been undertaken to convert lignin into activated carbon and apply it as an adsorbent for the removal of pollutants such as heavy metals from aqueous solution. These studies are summarized in the following section.

The removal of Cu(II) from aqueous solutions with Tunisian activated lignin prepared by phosphoric acid ($H_3PO_4$)was investigated by Kriaa *et al,* (2010). The authors investigated the adsorption of Cu(II) onto untreated natural lignin and lignin that was activated at 500$^oC$. Pores structure analysis, Boehm titration, TGA and FTIR were used to characterize the lignin samples. Batch adsorption experiments were performed to optimize the metal adsorption. The pH of the metal solutions was varied in the range 3-9 and the samples placed in a rotating shaker for 24 hours at 25$^oC$. The carbonization temperature was varied in the range 200-500$^oC$ and the lignin activated at a temperature of 500$^oC$ showed the highest specific surface area (564,5 $m^2/g$) but it resulted in the lowest yield (20,52%). An increase in carbonization temperature led to an increase in the adsorptive capacity of the activated carbon. At temperatures above 500$^oC$ the carbon structure shrinks and the surface area and pore volume decrease. An increase in pH led to an increase in the extent of adsorption and maximum adsorption was obtained at a pH of 6 an increase in pH beyond this point resulted in the decline in the extent of adsorption. The modification of natural lignin by means of activation with $H_3PO_4$ increased the surface area of

the lignin from 10 to 463,5 $m^2$/g because the surface structure of the raw material was changed. The equilibrium data was better described by the Langmuir isotherm model.

Gonzalez-Serrano *et al.,* (2004) studied the removal of water pollutants with activated carbons prepared from $H_3PO_4$ activation of lignin that was obtained from black liquors. The impregnation ratio (weight of $H_3PO_4$ relative to that of dry lignin) was varied from 1 to 3 and the activation temperature was varied from 350-600$^oC$. The pollutants that were used as adsorbates were phenol, 2,4,2-trichlorophenol and Cr(VI). The adsorption experiments were performed in batch mode by contacting an aqueous solution of adsorbate with a weighed sample of activated carbon in stoppered bottles placed in a thermostated shaker at 25$^oC$. The impregnation ratio did not show a significant effect on the BET surface area within the range tested but it affected the distribution of porosity. The activation temperature did not show a significant effect on the distribution of mesopore size. The relative adsorption capacity of the different carbons increased with the activation temperature and with the ratio, both of which are related to the widening of the porous structure. The adsorption capacity of the activated carbons towards chromium adsorption increased significantly at lower pH values (i.e. 3). This was attributed to the reduction of Cr(VI) to Cr(III) in the acidic pH range in the presence of activated carbons. The Langmuir equation provided a better fit of the equilibrium adsorption data. Optimum conditions for the preparation of the activated carbons were 2 g $H_3PO_4$/g lignin and 700$^oC$ for the impregnation ratio and temperature, respectively.

Activated carbon prepared from lignin by chemical activation has been studied by Hayashi *et al.* (2000). The main aim of the study was to investigate the influence of activating reagent on the pore structure and to determine the mechanism of activation. $K_2CO_3$, $Na_2CO_3$, KOH, NaOH, $ZnCl_2$ and $H_3PO_4$ were used as activating reagents. The impregnation ratios were 1.0 for all samples. The carbonization temperature was varied in the range 500-900$^oC$. The parameters that were used to compare the prepared carbons with commercial samples included the pore volumes and surface areas. The activated carbons prepared from lignin by chemical activation with $ZnCl_2$ and $H_3PO_4$ had surface areas as large as those of commercial activated carbons. At an activation temperature of 500$^oC$, the surface areas of activated carbons prepared using alkali metal compounds were very small compared with those of activated carbons prepared by $ZnCl_2$ and $H_3PO_4$ activation. The carbon prepared by $K_2CO_3$ activation had a surface area of 2000 $m^2/g$, which was larger than that of commercial activated carbons. The surface area reached a maximum value at a temperature of 800$^oC$ in alkali metal compound activation, and at a temperature of 600$^oC$with $ZnCl_2$ and $H_3PO_4$ activation. The pore volumes of activated carbons prepared by alkali metal compound activation increased with carbonization temperatures up to 800$^oC$. Above 800$^oC$ the excess enlargement induced combination of pores, resulting in an increase in mesopores for all alkali metal salts. This in turn results in the decrease of both the micropore volume and surface area.

In the next chapter, the methods used to carry out the experiments are discussed

# CHAPTER 3

# EXPERIMENTAL

## 3.1 INTRODUCTION

The procedures followed to carry out the experiments in batch mode in a stirred cell are discussed in the next sections. In this study the effects of operating pressure, membrane cut-off size, stirring rate and feed concentration on the extent of lignin retention and permeate flux were investigated.

## 3.2 MATERIALS

### 3.2.1 Chemicals and reagents

Black liquor was procured from a South African eucalyptus Kraft mill. The black liquor was diluted with deionised water to get the desired concentrations. Hydrophilic polyethersulfone membranes with molecular cut-off sizes of 5, 10 and 20 kDa were procured from Memcon (Pty) Ltd, South Africa. The membranes are usable in the pH range 0-14 and are resistant to temperatures up to 95$^{o}$C. The composition of the black liquor used is reported in Table 3.1 below

### 3.2.2 Instrumentation

- Thermostated water bath (Labotec)
- Thermostat vacuum oven (Townson & Mercer LTD)
- Peristaltic pump (323, Watson Marlow, South Africa)

- Stirred cell (Amicon 8400, Merck, South Africa)
- Magnetic stirrer with a digital display (MS-H280-Pro, Scilogex, USA)
- UV-Visible spectrophotometer (Varian CARY 50 CONC)

Table 3.1 Composition of the raw black liquor

| | |
|---|---|
| Lignin (g/L) | 44.02 |
| Total solids content (g/L) | 121.72 |
| Ash (%) | 9.02 |
| Hemicelluloses | % |
| Xylose | 0.03 |
| Arabinose | 0.15 |
| Galactose | 0.03 |
| Mannose | 0.00 |
| Glucose | 0.00 |

## 3.3 ULTRAFILTRATION STUDIES

### 3.3.1 Batch experiments

Ultrafiltration experiments were carried out to investigate the effect of three variables; transmembrane pressure (150, 250 and 350 kPa), stirring rate (200, 300 and 400 rpm) and feed concentration (3, 6 and 9 m/m%) on lignin retention and transient flux decline. One parameter was varied as the others were held constant to get an exact picture on dependence. All

experiments were conducted at 60$^{o}$C by circulating a heating water stream at 95$^{o}$C and 15 rpm in the coil around the stirred cell body. The disk membrane was placed on the porous support and the cell was assembled. Pure water flux at different transmembrane pressures was measured and plotted against the transmembrane pressure. The membrane resistance for each membrane was calculated from the slope of this plot. This was followed by the actual experiment by charging the cell with 200 mL of black liquor solution. The transmembrane pressure and stirrer speed were adjusted to desired levels using a pressure regulator and the speed controller on the magnetic stirrer, respectively. The duration of each experiment was one hour and permeate at different time intervals was measured by collecting 10 mL of permeate in a measuring cylinder and recording the time for this collection (Sarkar, 2013). The retentate was collected by opening the stirred cell after each run. The experiments were carried out in triplicates and average values were reported. After each run, the cell was dismantled and the membrane thoroughly washed with deionised water to remove any deposition. The membrane was soaked in distilled water overnight and pure water flux was checked again to observe any variation in its hydraulic resistance before its reuse. This procedure was repeated after every experiment.

3.3.1.1 Membrane hydraulic resistance

The hydraulic resistance of each membrane investigated was determined by recording the pure water flux as a function of pressure in the stirred cell and obtaining a linear relationship between the two parameters for each membrane. The membrane resistance $R_M$ can be calculated from Equation 3.1 (Schwarze et.al., 2010)

$$R_M = \frac{\Delta P}{\mu_W J_W} \qquad (3.1)$$

Where $\Delta P$ is the transmembrane pressure, $J_W$ is the pure water flux and $\mu_W$ is the viscosity of water with the effect of temperature taken into consideration.

3.3.1.2 Effect of membrane cut-off size

To investigate the effect of the cut-off size of the membrane, ultrafiltration was carried out in a stirred cell with three membranes that had cut-off sizes of 5, 10 and 20 kDa. For this study the feed concentration and stirring rate were fixed at 9% and 250rpm, respectively.

3.3.1.3 Effect of pressure

The effect of pressure was studied by varying the pressure in the range 150-350kPa while the stirring rate was fixed at 200rpm. For this study a 10 kDa membrane was used this was tested for feed concentrations 3, 6 and 9%.

3.3.1.4 Effect of feed concentration

For this study, a 10 kDa membrane was used and the stirring rate was fixed at 300 rpm for all experiments while the pressure was varied in the range 150-350kPa for each concentration point. This was tested at feed concentrations of 3, 6 and 9%.

3.3.1.5 Effect of stirring rate

The effect of the stirring rate was investigated in the range 200-400rpm while the pressure was fixed at 150 kPa while the feed concentration was varied in the range 3-9% for each stirring rate point.

3.4 Analysis

The total dissolved solids (TDS) concentrations were determined gravimetrically by evaporating a known volume of black liquor sample at 105$^{o}$C for 24 hours and determining the weight of the residue (Satyaranayana *et al*, 2000). The ash content is measured by heating the residue from the TDS measurement to 950$^{o}$C and weighing the sample afterwards (Dafinov *et al*, 2005). The ash content is indicative of the concentration of inorganic matter in the sample. Lignin can be measured from the light absorption at a wavelength of 280 nm as it contains phenolic groups which absorb light. A UV-Visible spectrophotometer (Varian CARY 50 CONC) was used to measure the UV light absorption of the black liquor samples to determine the lignin concentration. Where necessary, the samples were diluted with 0.1 M NaOH and an absorption constant of 24.6 L/g cm was used (Wallberg *et al*, 2003(a)). The hemicelluloses content of the black liquor was determined using a High Performance Liquid Chromatograph, comprising an autosampler (Perkin Elmer, Series 200), column oven (Perkin Elmer, Series 200), chromatography interface (Perkin Elmer, 600 Series), pulsed amperometric detector (Dionex) and analytical column (CarboPac PA-1, Dionex) (van Hazendonk *et al*, 1996).

The lignin retention in the stirred cell was calculated as follows (Britz, 2008):

$$R = \frac{\ln(c_R/c_F)}{\ln(VCF)} = \frac{\ln[VCF - (c_P/c_F)\,(VCF - 1)]}{\ln(VCF)} \qquad (3.2)$$

Where $c_F$, $c_P$ and $c_R$ are the feed, permeate and retentate concentrations (g/L), respectively.

Retention values calculated in this manner consider either the retentate or the permeate concentrations, and the corresponding VCF concentration ratio, allowing for comparison of retention values throughout the process. The volume concentration factor (VCF) is dimensionless and given as (Britz, 2008):

$$VCF = \frac{V_F}{V_R} \qquad (3.3)$$

$V_F$ and $V_R$ are the feed and retentate volumes, respectively. The VCF can be useful in the calculation of observed retention values of a solute during batch processes (Britz, 2008).

In the next chapter, the results will be presented and discussed.

# CHAPTER 4

# RESULTS AND DISCUSSION

## 4.1 INTRODUCTION

The aim of this experimental work was to investigate the feasibility of extracting lignin from black liquor by ultrafiltration on a bench scale using a stirred cell. The investigations evaluated the influence of membrane cut-off size, transmembrane pressure, feed concentration and stirring speed on the extent of lignin removal and permeate flux, and the results are reported and discussed in this chapter.

## 4.2. MEMBRANE CHARACTERIZATION

### 4.2.1. Membrane hydraulic resistance

The membrane resistance ($R_M$) results are presented in Table 4.1 below

Table 4.1 Membrane hydraulic resistances of all investigated membranes

| Membrane cut-off size (kDa) | $R_M$ ($10^{12}$ $m^{-1}$) |
|---|---|
| 5 | 14.5 |
| 10 | 5.08 |
| 20 | 3.39 |

From Table 4.1 it was observed that the membrane resistance increased with decreasing cut-off of the membrane. This was expected because for membranes with lower molecular weight cut off, the pore sizes become constricted and a reduction in flux is expected.

## 4.3 BATCH ULTRAFILTRATION TEST RESULTS

### 4.3.1 Membrane selection

Ultrafiltration was carried out in a stirred cell with three membranes that had cut-off sizes of 5, 10 and 20 kDa. This is because black liquor is a polydispersed solution that has a wide range of molecular weight (and size) distribution of solutes ranging from 100 to 100 000 (Satyanarayana *et al*, 2000): therefore, the selection of a membrane cut-off size is important for the efficiency of the process. Lignin retention with pressure and the variation of flux with time for different membranes are represented by Figures 4.1 and 4.2, respectively. For this study the feed concentration and stirring rate were fixed at 9% and 250 rpm, respectively. The maximum retention and flux values which were achieved in this study did not represent the real optimum values because the variation of other variables such as concentration and stirring rate were not considered. From Figure 4.1, it is shown that retention increased as the membrane with a lower cut-off size is used. For instance, at a transmembrane pressure of 150 kPa, retention was 83.87% for the 5kDa membrane, whereas under the same experimental conditions, that for the 20 kDa membrane was 56.09%. The same trend is observed for the entire pressure range tested. This is because for membranes with higher cut-off sizes more solutes that have sizes less than the pore size of that particular membrane tend to pass through, thereby decreasing retention of the more open membrane.

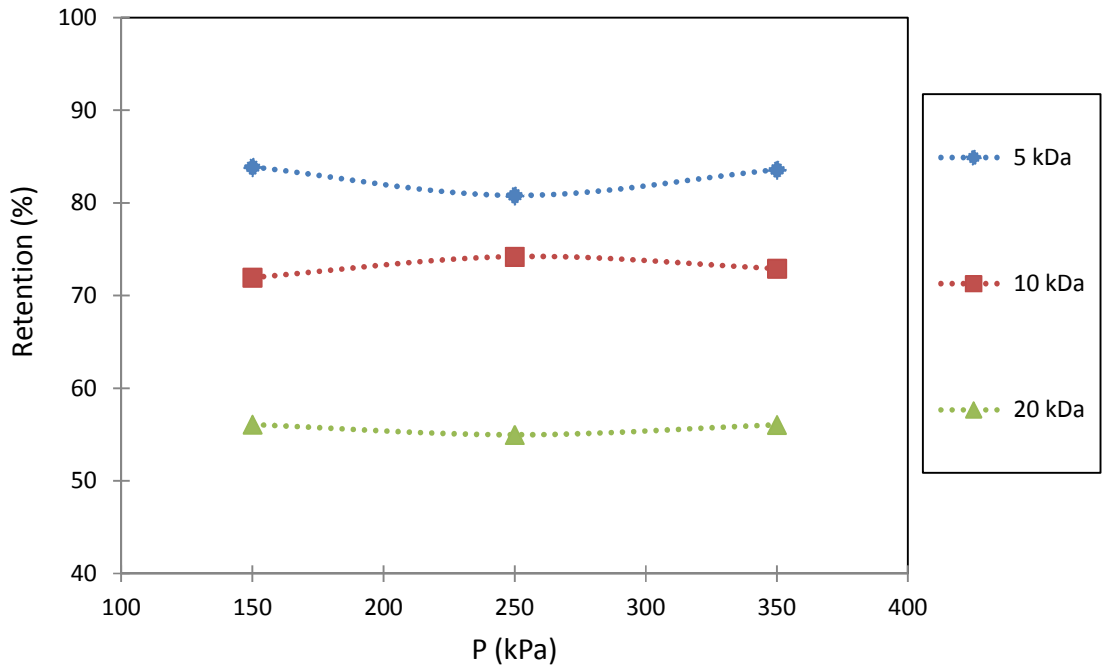


Figure 4.1 Variation of lignin retention with pressure for different membranes in a stirred cell. $C_o$ = 9% and ω = 250 rpm

The initial permeate flux, as shown in Figure 4.2, was found to be comparatively higher for membranes with higher cut-off sizes for an operating pressure of 150 kPa. The initial permeate flux for the 5kDa membrane was comparatively lower at 15.11 L/m$^2$ hr and it remained fairly constant throughout the course of the run. For the 10kDa membrane it was 33.12 L/m$^2$ hr, which was a 2-fold increase in flux compared to the 5kDa membrane. This flux was maintained at 33.12 L/m$^2$ hr for 30 minutes and started to decrease gradually after that time period. For the 20kDa membrane it was 47.85 L/m$^2$ hr (almost 45% increase compared to the 10kDa membrane) and it could only be maintained for 20 minutes after which it started to decrease rapidly during the course of the run. The gradual decline in permeate flux for the 10 and 20 kDa membranes can

be attributed to the deposition of the solute particles in the membranes pores as well as build up of deposited layer on the membrane surface. The combined effects of these results in reduction of permeate flux during the course of operation (Satyanarayana *et.al*, 2000). Although the 5 kDa size membrane had the highest retention, its flux was too low for a comparative study. Therefore, to investigate the effect of operating parameters on both the flux and retention a 10 kDa size membrane was used.

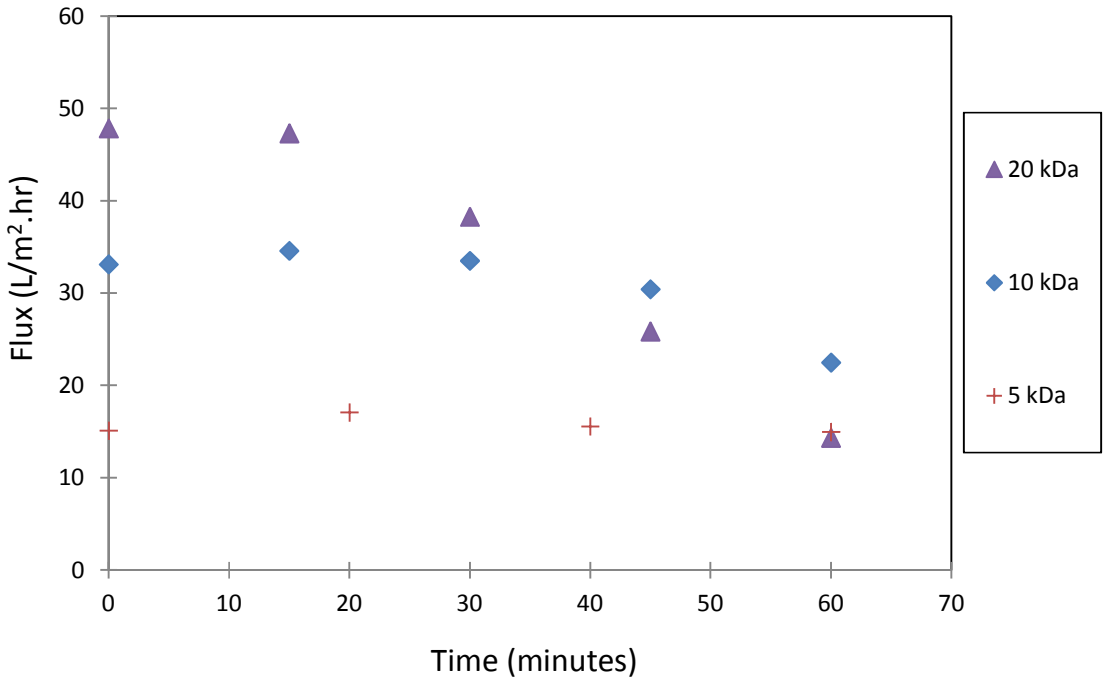


Figure 4.2 Variation of permeate flux as a function of time for different membranes in a stirred cell.

### 4.3.2 Effect of Pressure

Figures 4.3(a), (b) and (c) represent the effect of pressure on lignin retention at stirring rates of 200, 300 and 400 rpm, respectively. Figures 4.3(a), (b) and (c) are each plotted for feed concentrations 3, 6 and 9%. An increase in pressure from 150 to 250 kPa, as shown in Figure 4.3(a), resulted in only a marginal increase in the retention of lignin of less than 2% for the entire concentration range tested. However, for the 6 and 9% solutions, from Figure 4.3(a), as the pressure was increased further from 250 to 350 kPa the retention increased from 60.65 to 67.31% and from 73.77 to 79.53%, respectively. The same trend was observed for experiments conducted at stirring rates of 300 and 400 rpm, as shown in Figures 4.3(b) and (c). This was attributed to the fact that as the pressure is increased the convective diffusion of solutes to the membrane surface is increased, which in turn results in severe concentration polarization. This leads to an increase in viscosity of the solution near the membrane surface as the higher molecular weight organics are retained by the membrane and this viscous layer is responsible for pre-sieving of the organic solutes (De and Bhattacharya, 1996).

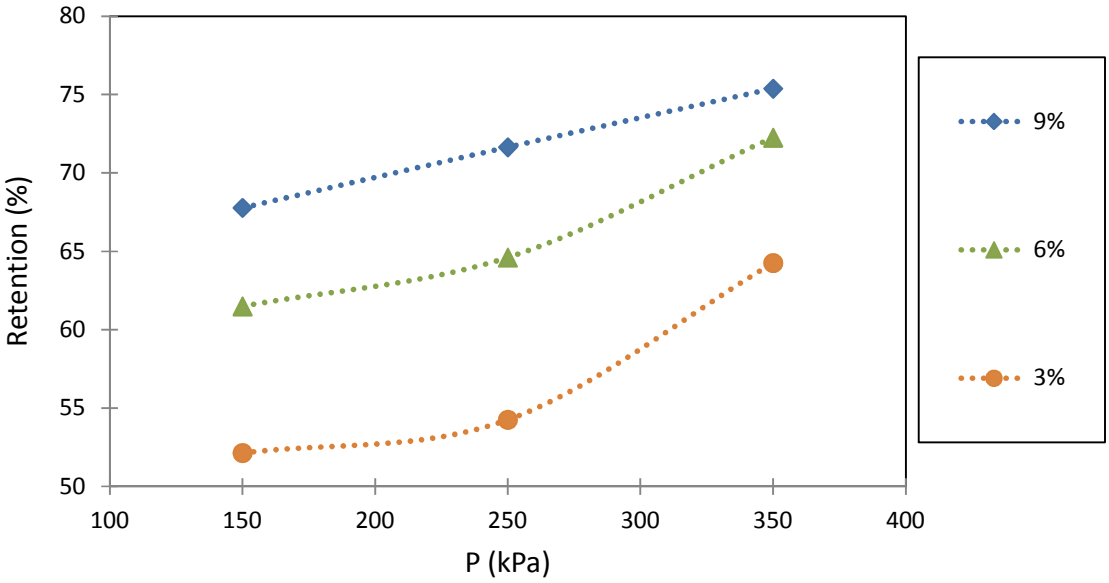


Figure 4.3(a) Variation of lignin retention with pressure for different feed concentrations in a stirred cell. Membrane size = 10 kDa, Stirring speed = 200 rpm

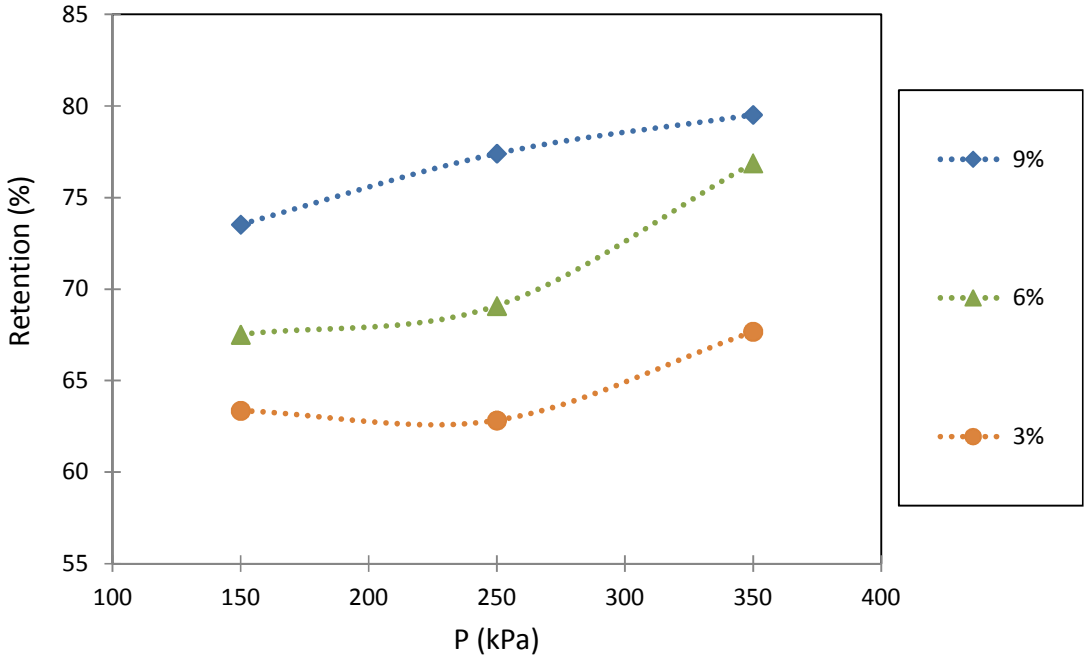


Figure 4.3(b) Variation of lignin retention with pressure for different feed concentrations in a stirred cell. Membrane size = 10 kDa, Stirring speed = 300 rpm

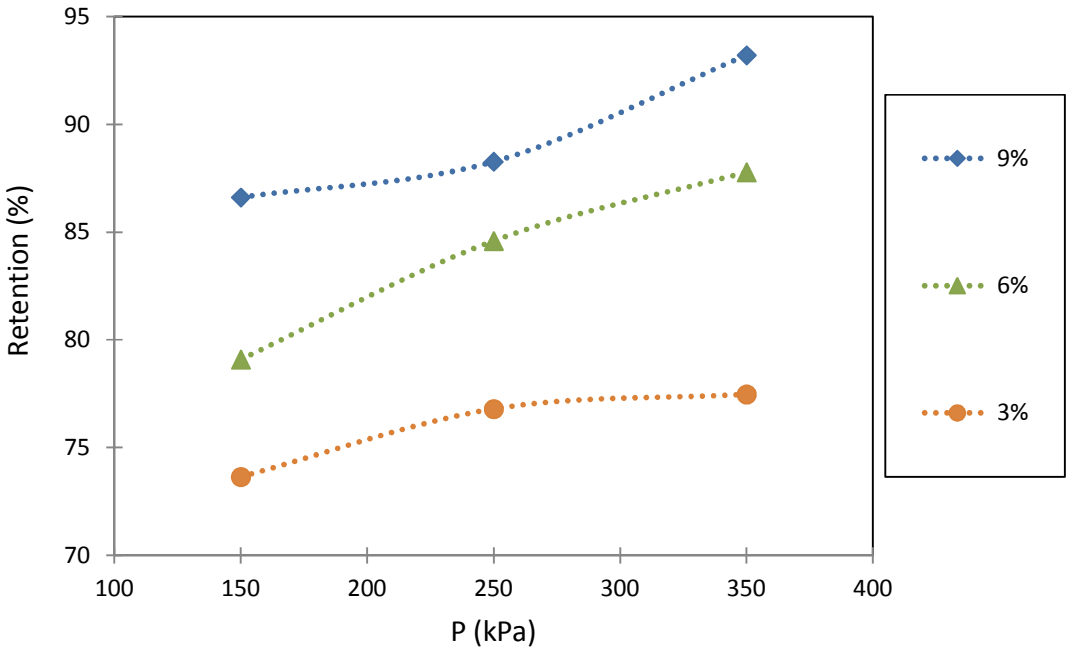


Figure 4.3(c) Variation of lignin retention with pressure for different feed concentrations in a stirred cell. Membrane size = 10 kDa, Stirring speed = 400 rpm

The variation of permeate flux with time at different pressures is presented in Figure 4.4. For this study the feed concentration and stirring rate were fixed at 6% and 200 rpm, respectively. The flux values which were achieved in this study did not represent the real optimum values because the variation of other variables such as concentration and stirring rate were not considered. The high initial permeate flux values at higher pressures, as shown in Figure 4.4, are as a result of increase in driving force of solvent through the membrane. However the decrease in permeate flux during the course of operation is rapid for higher pressures. For ultrafiltration at 350 kPa, after 20 minutes, the flux declined by 83% from 50.66 to 27.65 whereas that for ultrafiltration at 250 kPa declined by 38% from 41.01 to 29.70 in the same time interval. For ultrafiltration at 150 kPa, after 20 minutes only a 17% decline in permeate flux from 28.05 to 23.92% was observed. This is because the rate of deposition of solutes on the membrane surface occurs at a faster rate

as the pressure is increased. This reduces the net driving force of the solvent transport through the membrane as a result of the increase in osmotic pressure of the solution at the surface. Furthermore, the deposited layer becomes compact at higher pressures and this increases the resistance against solvent (Satyanarayana *et al*, 2000; De and Bhattacharya, 1996; Noordman, 2002).

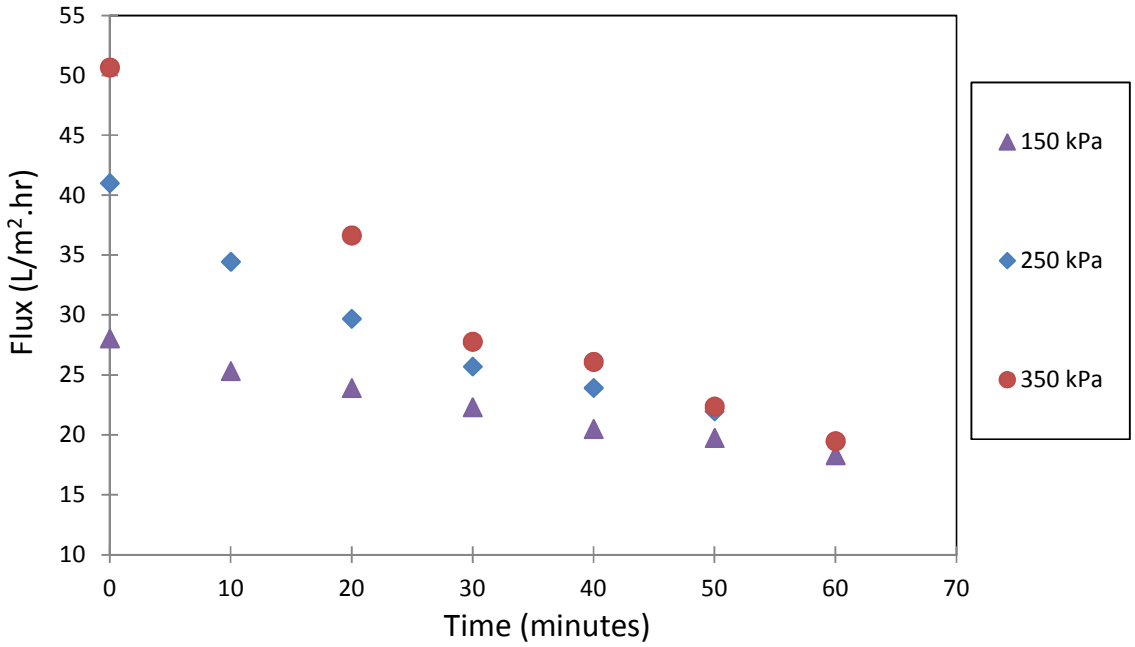


Figure 4.4 Variation of permeate flux as a function of time for different pressures in a stirred cell. Feed concentration = 6%, Membrane size = 10 kDa, Stirring speed = 200 rpm

### 4.3.3 Effect of feed concentration

The effect of black liquor feed concentration on the extent of retention is described in Figures 4.5(a), (b) and (c) for stirring rates of 200, 300 and 400 rpm, respectively. The retention of lignin in the stirred cell increased with an increase in feed concentration in the entire range tested, as

shown in Figures 4.5(a), (b) and (c). For instance, as shown in Figure 4.5(a) at an operating pressure of 350 kPa, an increase in feed concentration from 3 to 9% resulted in an increase in retention from 57.61 to 79.53%, respectively. For an operating pressure of 250 kPa, on the same plot, the extent of retention increased from 53.68 to 73.51% as the feed concentration was increased in the same range. The same trend was observed for experiments conducted at stirring rates of 300 and 400 rpm, as shown in Figures 4.5(b) and (c).

This can be explained by the fact that as the ultrafiltration process proceeds, the viscosity of the solution near the membrane surface increases as a result of organic solutes that are rejected by the membrane (De and Bhattacharya, 1996). This layer serves to sieve organic solutes. Because the viscosity of black liquor is dependent on its concentration, increasing the feed concentration of the solution results in an increase of the rate of formation of the viscous layer near the membrane surface as well as its viscosity. Black liquor components have molecular weight (and size) distribution ranging from 100 to 100 000 Da. Therefore when a viscous layer is formed near the membrane surface, the retention of low molecular weight lignin fractions that would under normal circumstances permeate through the membrane are retained, thus increasing the retention (Satyanarayana *et.al.*, 2000).

The same trend was observed for other operating pressures tested but it has to be highlighted that at a constant feed concentration higher operating pressures resulted in higher retention values. For example, from Figure 4.5(a), at a fixed feed concentration of 6%, increasing the pressure from 250 to 350 kPa resulted in an increase in retention from 60.65 to 67.32%. This is because at a higher pressure the viscous layer formed at the membrane surface becomes more compact which enhances its ability to sieve low molecular weight lignin fractions (De and Bhattacharya, 1996; Satyanarayana *et.al.*, 2000)

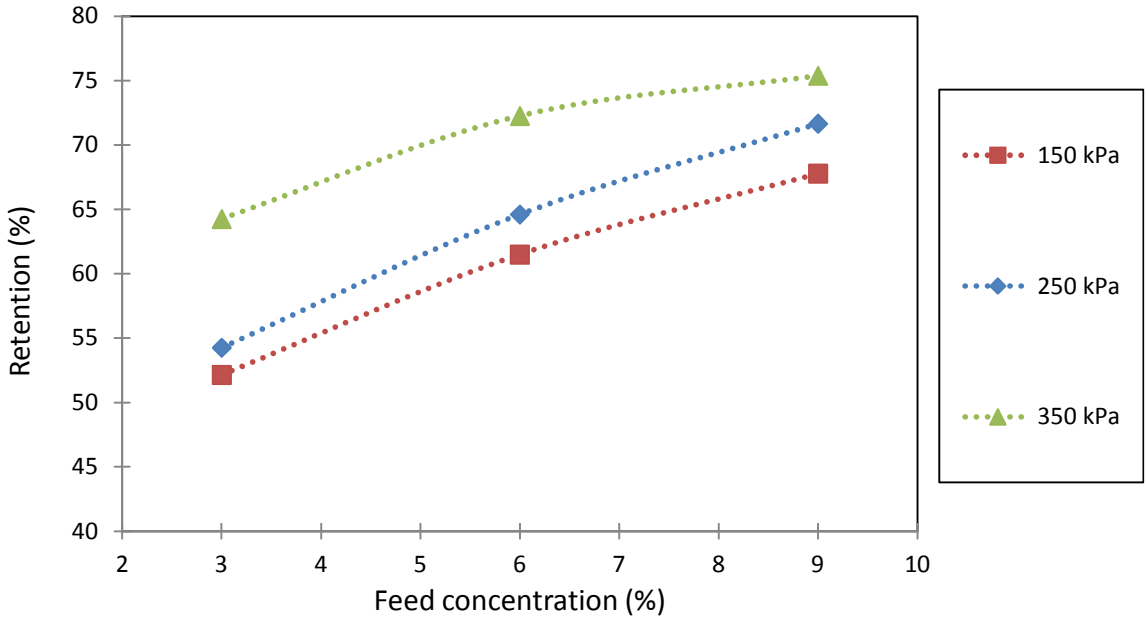


Figure 4.5(a) Variation of lignin retention with feed concentration for different pressures in a stirred cell. Stirring speed = 200 rpm, Membrane size = 10 kDa

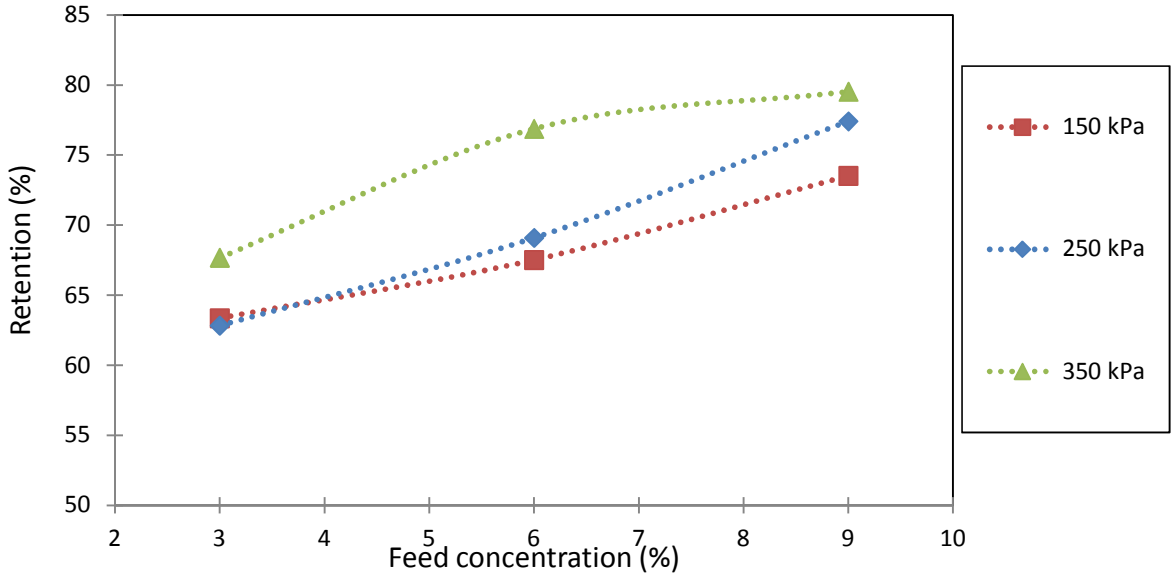


Figure 4.5(b) Variation of lignin retention with feed concentration for different pressures in a stirred cell. Stirring speed = 300 rpm, Membrane size = 10 kDa

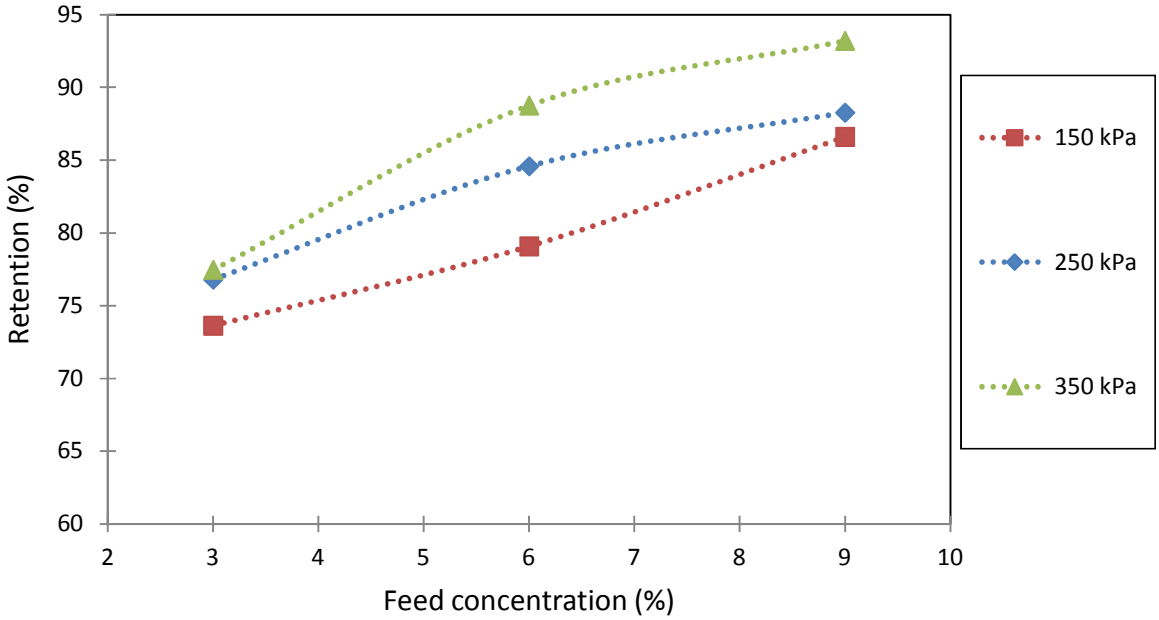


Figure 4.5(c) Variation of lignin retention with feed concentration for different pressures in a stirred cell. Stirring speed = 400 rpm, Membrane size = 10 kDa

The variation of permeate flux as a function of time for different feed concentrations is displayed in Figure 4.6. This was plotted for transmembrane pressure and stirring rate values of 250 kPa and 300 rpm, respectively. The flux values which were achieved in this study did not represent the real optimum values because the variation of other variables such as pressure and stirring rate were not considered It was observed that the initial permeate flux, as shown in Figure 4.6, was comparatively higher for less concentrated solutions. The initial flux readings were 95.69, 62.86 and 44.17 L/m$^2$ hr for the 3, 6 and 9% solutions, respectively. The variation with initial flux as a function of feed concentration is as a result of osmotic pressure resistance which is established within seconds of operation and this resistance is strongly dependent on feed concentration (De and Bhattacharya, 1996). The reduction in flux with an increase in feed concentration is because the bulk concentration in the stirred cell increases as the solutes are rejected by the membrane

which in turn increases the extent of solute deposition near the membrane surface. The flux is reduced as the resistance to solvent transport through the membrane is increased in the polarized layer (Bhattacharjee and Datta, 1997). It is worth noting from Figure 4.6 that after a filtration duration of 20 minutes, the permeate flux for the 6 and 9% solution reached the same value and decreased at the same rate until the end of the filtration run. Also after 40 minutes the same flux reading was recorded for all solutions tested which indicates the same magnitude of total resistance to flow. For the 3% solution the rate of depletion of solvent in the stirred cell is comparatively higher which results in the accelerated build-up of deposited layer, hence the flux reaches the same value as that of the 6 and 9% solutions. For the 6 and 9% solutions the osmotic pressure is comparatively higher due increased concentration which retards the rapid depletion of the solvent from the stirred cell, hence the flux decreases gradually with time.

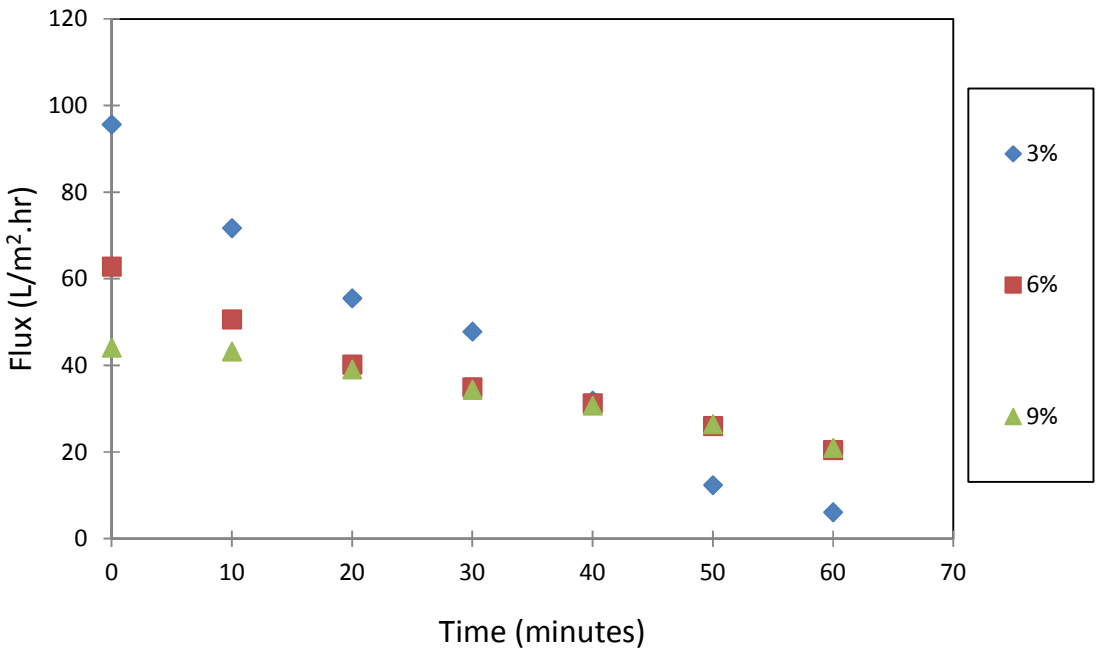


Figure 4.6 Variation of permeate flux as a function of time for different feed concentrations in a stirred cell. Pressure = 250 kPa, Stirring speed = 300 rpm, Membrane size = 10 kDa

### 4.3.4 Effect of stirring rate

The effect of stirring rate on the extent of retention is described in Figures 4.7(a), (b) and (c) for transmembrane pressure values of 150, 250 and 350 kPa, respectively. From Figures 4.7(a), (b) and (c) it is shown that as the stirring rate is increased, there is a corresponding increase in lignin retention in the entire concentration range investigated. For a transmembrane pressure of 150 kPa, as the stirring rate was increased from 200 to 400 rpm, as shown in Figure 4.7(a), there was a corresponding increase in retention from 59.94 to 73.64% for the 3% solution. For the 6 and 9% solutions, from the same plot, the extent of retention increased from 61.50 to 79.10% and from 67.78 to 86.61%, respectively. The same trend was observed for experiments conducted at transmembrane pressure values of 250 and 530 kPa, as shown in Figures 4.7(b) and (c)

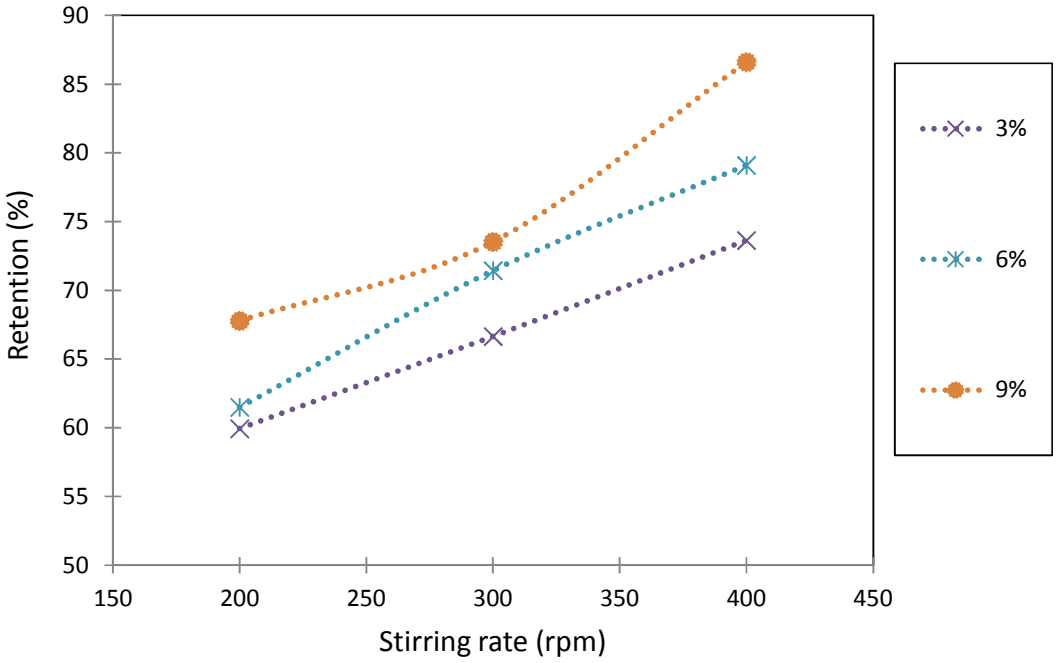


Figure 4.7(a) Variation of lignin retention with stirring rate for feed concentrations in a stirred cell. Pressure = 150 kPa, Membrane size = 10 kDa

A possible explanation for this observation is that at a low stirring speed the rate of diffusion of solutes from the membrane surface to the bulk solution is comparatively lower due to the significant reduction in the influence of external forced convection that is induced by stirring. Since black liquor is a polydispersed solution, there is a possibility that lignin fractions with molecular weight sizes that are less than the cut-off size of the membrane permeate through the membrane, thus reducing the extent of retention. The backward diffusion of solute from the membrane surface to the bulk is enhanced as the stirring rate in the stirred cell is increased and forced convection of solutes prevents them from being deposited on the membrane surface. This in turn minimizes the possibility of the low molecular weight lignin fractions from permeating through thus increasing the extent of retention.

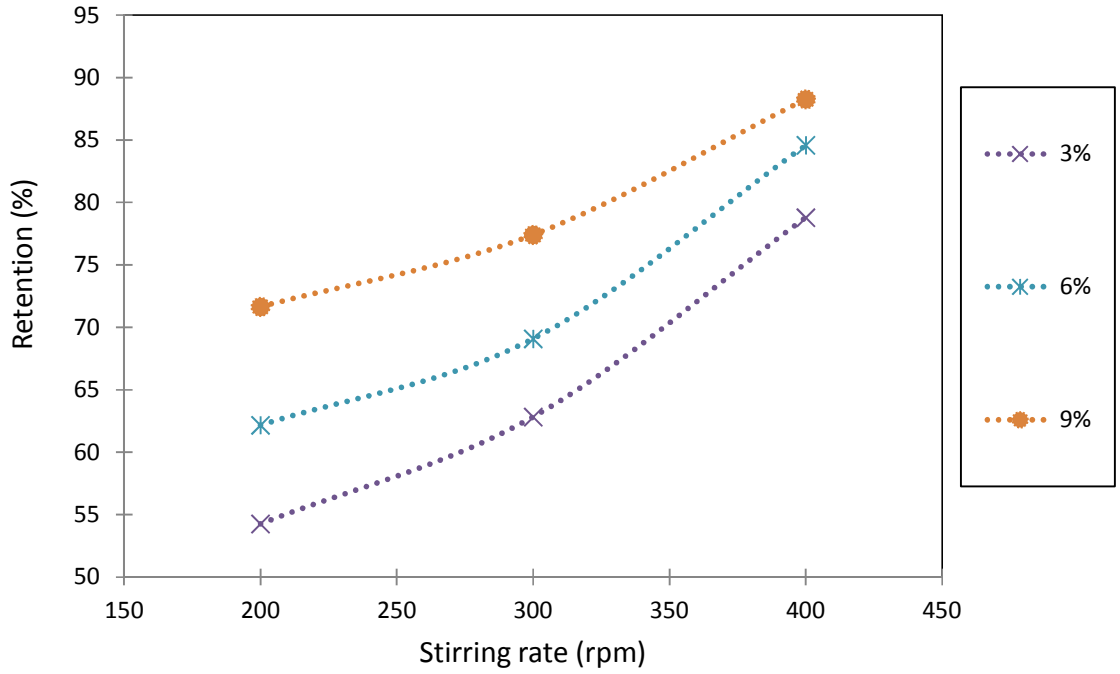


Figure 4.7(b) Variation of lignin retention with stirring rate for feed concentrations in a stirred cell. Pressure = 250 kPa, Membrane size = 10 kDa

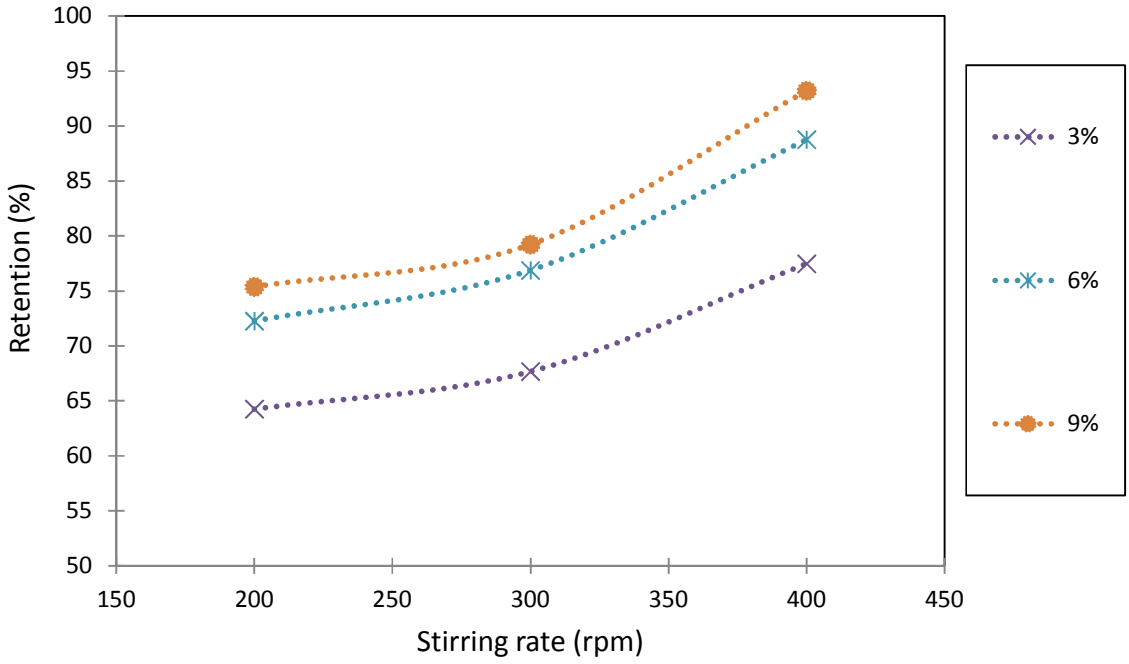


Figure 4.7(c) Variation of lignin retention with stirring rate for feed concentrations in a stirred cell. Pressure = 350 kPa, Membrane size = 10 kDa

The variation of flux as a function of time at different stirring rates is represented by Figure 4.8. This study was conducted with a solution that had a feed concentration of 3% at an operating transmembrane pressure of 150 kPa. The flux values which were achieved in this study did not represent the real optimum values because the variation of other variables such as concentration and pressure were not considered. As the stirring rate is increased from 200 to 300 rpm, as shown in Figure 4.8, the initial permeate flux increased from 55.21 to 81.25 L/m$^2$ hr. This is because as the rate of backward diffusion of solutes from the membrane surface to the bulk is enhanced by an increase in stirring rate, there is less build up of osmotic pressure and the effective pressure difference is more resulting in an increase in flux (Satyanarayana *et al*, 2000).

It is worth noting that in the 20-40 minute time interval the fluxes for 300 and 400 rpm are approximately equal to each other, indicating that the extent of minimization of osmotic pressure at the membrane surface is approximately the same as the stirring rate is increased above 300 rpm. This means the resistance to permeation of the solvent is approximately the same in that specific time interval. The rapid decline in permeate flux for stirring rates of 300 and 400 rpm is as a result of increase in the bulk solution viscosity which increases osmotic pressure (the extent of increase is minimized by stirring) as the solvent permeates through the membrane at a faster rate compared to 200 rpm. This is substantiated by the significant deviation in flux values for 300 and 400 rpm in the 50-60 minute time interval. This indicates that the resistance to solvent flow for 300 rpm increases as a result of the slower back diffusion of solute from the membrane surface as the viscosity and concentration of the solution increases. For 400 rpm this effect is offset by the faster rate of back diffusion of solute from the surface, which minimizes the increase in osmotic pressure/resistance.

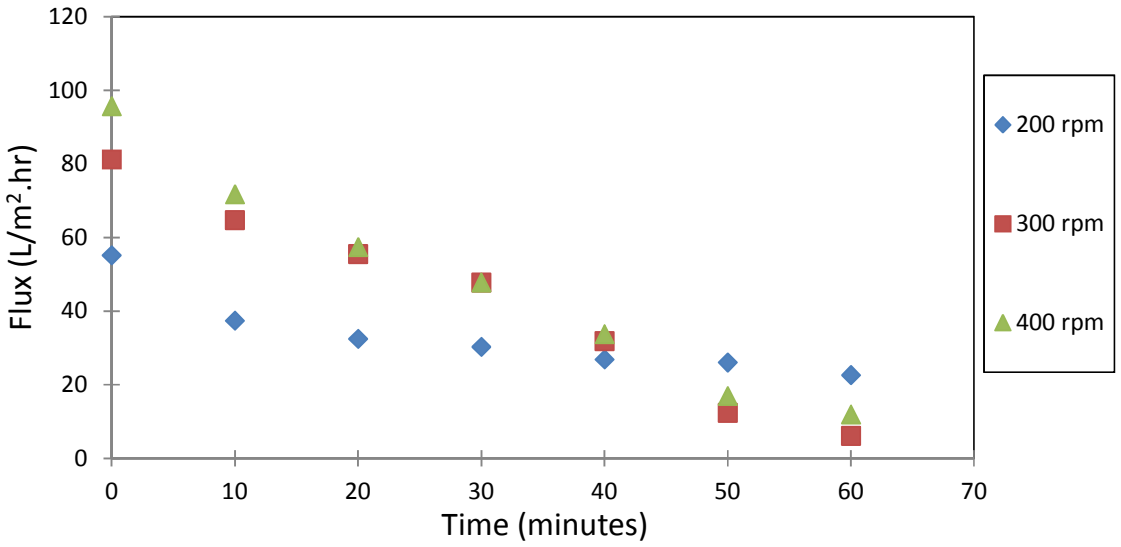


Figure 4.8 Variation of permeate flux as a function of time for different stirring rates in a stirred cell. Pressure = 150 kPa, Feed concentration = 3%, Membrane size = 10 kDa

### 4.3.5 Ash and solids content analysis

Tables 4.2, 4.3, 4.4, 4.5 represent the ash content analysis results of the fractions collected at the end of the ultrafiltration runs, respectively. All experiments, except for the membrane selection study, were carried out using the 10 kDa membrane. An optimum membrane cut-off size should result in minimal retention of cooking chemicals, (i.e., sodium and sulphur). In addition to the fact that they have to be reused in the cooking process, this is necessary to avoid forming ash and sulphur dioxide when these inorganic elements are combusted in a normal furnace (Wallberg *et al*, 2003a). The increase in ash content in the retentate fractions is as a result of the retention of multivalent ions that are associated with the retained organic matter. For example, for the 5kDa membrane and an operating transmembrane pressure of 150kPa as observed in Table 4.2, the ash content increased from 5.78 (raw) to 7.09% (retentate stream). The same trend was observed for all different combinations of membrane cut-off size and process conditions as reported in Tables 4.4, 4.6 and 4.8. This was also observed by Wallberg at al (2003)(a) and Wallberg at al (2003)(b) when they used polymeric and ceramic membranes to fractionate and concentrate black liquor. The ash that is observed in the permeate streams is attributed to monovalent ions as their retention is insignificant.

Table 4.2 Ash content analysis of ultrafiltration fractions from the membrane selection study

| Pressure (kPa) | Membrane cut-off size (kDa) | | | | | |
|---|---|---|---|---|---|---|
| | 5 | | 10 | | 20 | |
| | Ash Content (%) | | Ash Content (%) | | Ash Content (%) | |
| | Permeate | Retentate | Permeate | Retentate | Permeate | Retentate |
| 150 | 4.14 | 7.09 | 4.61 | 8.85 | 5.5 | 9.49 |
| 250 | 4.27 | 8.83 | 4.7 | 8.7 | 4.52 | 11.22 |
| 350 | 3.9 | 8.75 | 4.61 | 10.46 | 4.82 | 12.07 |

Table 4.3 Ash content analysis of ultrafiltration fractions from the pressure variation study

| Feed Concentration (%) | Pressure (kPa) | | | | | |
|---|---|---|---|---|---|---|
| | 150 | | 250 | | 350 | |
| | Ash Content (%) | | Ash Content (%) | | Ash Content (%) | |
| | Permeate | Retentate | Permeate | Retentate | Permeate | Retentate |
| 3 | 1.22 | 1.73 | 0.56 | 3.16 | 0.44 | 4.11 |
| 6 | 3.11 | 4.78 | 2.75 | 5.22 | 2.11 | 7.27 |
| 9 | 4.47 | 7.56 | 4.89 | 7.39 | 4.98 | 8.24 |

Table 4.4 Ash content analysis of ultrafiltration fractions from the concentration variation study

| Pressure (kPa) | Feed Concentration (%) | | | | | |
|---|---|---|---|---|---|---|
| | 3 | | 6 | | 9 | |
| | Ash Content (%) | | Ash Content (%) | | Ash Content (%) | |
| | Permeate | Retentate | Permeate | Retentate | Permeate | Retentate |
| 150 | 0.6 | 6.4 | 3.41 | 4.86 | 4.27 | 8.76 |
| 250 | 4.33 | 10.55 | 2.16 | 8.12 | 4.78 | 9.94 |
| 350 | 0.62 | 11.02 | 1.7 | 6.68 | 3.74 | 11.23 |

Table 4.5 Ash content analysis of ultrafiltration fractions from the stirring rate variation study

| Feed Concentration (%) | Stirring rate (rpm) | | | | | |
|---|---|---|---|---|---|---|
| | 200 | | 300 | | 400 | |
| | Ash Content (%) | | Ash Content (%) | | Ash Content (%) | |
| | Permeate | Retentate | Permeate | Retentate | Permeate | Retentate |
| 3 | 1.22 | 1.73 | 0.6 | 6.4 | 1.17 | 4.85 |
| 6 | 3.11 | 4.78 | 3.41 | 4.86 | 2.36 | 3.78 |
| 9 | 4.47 | 7.56 | 4.27 | 8.76 | 3.71 | 6.45 |

Tables 4.6, 4.7, 4.8, 4.9 represent the solids content analysis results of the fractions collected at the end of the ultrafiltration runs, respectively. All experiments, except for the membrane selection study, were carried out using the 10 kDa membrane. For example, for the 10 kDa membrane and an operating transmembrane pressure of 250kPa, as recorded in Table 4.6, the solids content increased from 8.48 (raw) to 12.91% (retentate stream). The retention of solids during ultrafiltration is increased by the reduction in cut-off size of the membrane (Toledano *et al.*, 2010). The same trend (i.e. the concentration of solids in the retentate stream) was observed for all different combinations of membrane cut-off size and process conditions as reported in Tables 4.7, 4.8 and 4.9.

Table 4.6 Solids content analysis of ultrafiltration fractions from the membrane selection study

| Pressure (kPa) | Membrane cut-off size (kDa) | | | | | |
|---|---|---|---|---|---|---|
| | 5 | | 10 | | 20 | |
| | Solids Content (%) | | Solids Content (%) | | Solids Content (%) | |
| | Permeate | Retentate | Permeate | Retentate | Permeate | Retentate |
| 150 | 5.55 | 9.54 | 5.37 | 11.18 | 6.55 | 13.78 |
| 250 | 4.73 | 12.72 | 5.45 | 12.91 | 6.17 | 16.12 |
| 350 | 4.94 | 14.54 | 5.6 | 15.38 | 6.21 | 17.72 |

Table 4.7 Solids content analysis of ultrafiltration fractions from the pressure variation study

| Feed Concentration (%) | Pressure (kPa) | | | | | |
|---|---|---|---|---|---|---|
| | 150 | | 250 | | 350 | |
| | Solids Content (%) | | Solids Content (%) | | Solids Content (%) | |
| | Permeate | Retentate | Permeate | Retentate | Permeate | Retentate |
| 3 | 1.19 | 2.77 | 0.82 | 4.41 | 0.3 | 8.38 |
| 6 | 3.63 | 7.06 | 3.47 | 8.32 | 4.01 | 8.75 |
| 9 | 7.07 | 11.55 | 6.84 | 11.82 | 6.72 | 13.32 |

Table 4.8 Solids content analysis of ultrafiltration fractions from the concentration variation study

| Pressure (kPa) | Feed Concentration (%) | | | | | |
|---|---|---|---|---|---|---|
| | 3 | | 6 | | 9 | |
| | Solids Content (%) | | Solids Content (%) | | Solids Content (%) | |
| | Permeate | Retentate | Permeate | Retentate | Permeate | Retentate |
| 150 | 2.48 | 12.67 | 4.86 | 9.25 | 7.14 | 12.23 |
| 250 | 1.97 | 15.04 | 4.93 | 11.7 | 6.83 | 14.9 |
| 350 | 2.09 | 15.7 | 4.66 | 12.02 | 6.64 | 16.31 |

Table 4.9 Solids content analysis of ultrafiltration fractions from the stirring rate variation study

| Feed Concentration (%) | Stirring rate (rpm) | | | | | |
|---|---|---|---|---|---|---|
| | 200 | | 300 | | 400 | |
| | Solids Content (%) | | Solids Content (%) | | Solids Content (%) | |
| | Permeate | Retentate | Permeate | Retentate | Permeate | Retentate |
| 3 | 1.19 | 2.77 | 2.48 | 12.67 | 2.19 | 7.22 |
| 6 | 3.63 | 7.06 | 4.86 | 9.25 | 4.94 | 9.45 |
| 9 | 7.07 | 11.55 | 7.14 | 12.23 | 5.87 | 10.25 |

# CHAPTER 5

# MODELLING

## 5.1. INTRODUCTION

The flux decline experimental data was modelled by applying the solute mass balance for a stirred cell and by assuming that fouling mechanism is described by the intermediate blocking model. With the intermediate blocking model it is assumed that foulants reaching the membrane directly block some membrane area or deposit on other already deposited fouling particles. The total resistance was expressed using a resistance-in-series model based on Darcy's law. A model for constant pressure dead-end filtration laws was proposed by Sarkar (2013) to analyze the flux decline during ultrafiltration in a batch cell. The proposed model was based on Hermia's classic filtration laws and sequential occurrence of complete pore blocking and cake filtration mechanisms and the model predicted results were successfully compared with the experimental data. The modelling procedure used by the author was adapted for this work but only one mechanism (intermediate blocking) was considered as opposed to the two mechanisms considered by the author.

## 5.2. STIRRED CELL ULTRAFILTRATION DATA MODELLING

The solute mass balance in the cell is given as (Sarkar, 2013):

$$\frac{d(V_f C_b)}{dt} = -J(t) A C_p \qquad (5.1)$$

A is the effective membrane area and $V_f$ is the volume of retentate at any time, t, during the experiment, respectively.

According to Sarkar (2013), the variation of retentate volume with time can be obtained by writing the material balance in the cell as (that is by assuming that the solution retained within the pores of the accumulating cake volume on the membrane surface is negligible):

$$\frac{d(V_f \rho_b)}{dt} = -J(t) A \rho_p \qquad (5.2)$$

where $\rho_f$ and $\rho_p$ are the densities of retentate and permeate. Assuming $\rho_f \cong \rho_p$ the above equation can be written as (Sarkar, 2013)

$$\frac{dV_f}{dt} = -JA \qquad (5.3)$$

The initial conditions are given by at $t = 0,\ V_f = V_0$ and $C_b = C_0$

The variables can be normalized as (Sarkar, 2013):

$$C_{bd} = \frac{C_b}{C_0};\quad \tau = \frac{tD}{R^2};\ v = \frac{AR}{V_0}\ ;\ F = \frac{JR}{D};\quad V_{fd} = \frac{V_f}{V_0}$$

where R and D are the radius of cell and solute diffusivity, respectively.

Equation 5.1 can be written as (Sarkar, 2013):

$$\frac{dC_{bd}}{d\tau} = \frac{F(\tau) v C_{bd}}{V_{fd}} \qquad (5.4)$$

Whereas Equation 5.3 can be written as (Sarkar, 2013):

$$\frac{dV_{fd}}{dt} = -F(\tau)v \qquad (5.5)$$

The dimensionless form of the initial conditions of Equations 5.4 and 5.5 can be expressed as (Sarkar, 2013):

At $\tau = 0, \quad C_{bd} = 1, \quad V_{fd} = 1$

The governing equation of flux decline due to pore blocking for constant pressure filtration can be represented from Hermia's law as (Iritani, 2013):

$$\frac{dJ}{dt} = -kJ^{3-n} \qquad (5.6)$$

The two constants $k$ and $n$ depend on the mode of filtration and the blocking index $n$ is a dimensionless filtration constant that characterizes the mode of fouling model involved. It is assumed that the intermediate blocking law best describes the fouling mechanism of the ultrafiltration process therefore $n = 1$ and Equation 5.6 can be written as (Sarkar, 2013; Iritani, 2013):

$$\frac{dJ}{dt} = -kJ^2 \qquad (5.7)$$

The solution for Equation 5.7 is given as (Iritani, 2013):

$$J = \frac{J_0}{k_i J_0 t + 1} \qquad (4.8)$$

where $k_i$ is the intermediate blocking constant

In dimensionless form, Equation 5.8 can be written as:

$$F(\tau) = \frac{F_0}{k_1 F_0 \tau + 1} \qquad (5.9)$$

where $k_1 = k_i R$ ; $F_0 = \frac{J_0 R}{D}$ and $J_0 = \Delta P / \mu R_m$ is the initial permeate flux

The membrane hydraulic resistance as well as the intermediate fouling can be considered as two resistances in series of a resistance-in-series model based on Darcy's law. The filtration rate $J$ is related to the filtration resistance and transmembrane pressure as (Sarkar, 2013):

$$J = \frac{\Delta P}{\mu_p R_t} = \frac{\Delta P}{\mu(R_m + R_i)} \qquad (5.10)$$

In dimensionless form Equation 5.10 can be written as (Sarkar, 2013):

$$F(\tau) = \frac{F_0}{1 + R_{id}} \qquad (5.11)$$

where $R_{id}$ is the dimensionless intermediate resistance. $R_{id}$ is expressed in terms of intermediate blocking resistance $R_i$ and membrane hydraulic resistance $R_m$ as $R_{id} = R_i / R_m$

From Equations 5.9 and 5.11, the dimensionless intermediate resistance $R_{id}$ can be expressed as:

$$R_{id} = k_1 F_0 \tau \qquad (5.12)$$

5.2.1. Estimation of model parameter $k_i$

- From the knowledge of membrane permeability and operating transmembrane pressure, dimensionless pure water flux ($F_0$) is calculated. Next, the value of $k_i$ is guessed.

- At various operating time, permeate flux values $J_{cal}$ and dimensionless intermediate resistance $R_{id}$ values are calculated by solving the coupled differential and algebraic equations, Equations 5.4, 5.5, 5.8 and 5.12 using the POLYMATH® 5.1 software (utilizing using the STIFF method) with the following initial condition, at $\tau = 0, \quad C_{bd} = 1, \quad V_{fd} = 1$

- If convergence is not achieved, another value of $k_i$ is chosen and step 2 is repeated until the required convergence is achieved. The profiles of permeate flux and dimensionless intermediate resistance are obtained as a function of time and the $k_i$ values are recorded.

Table 5.1 below represent the $k_i$ values estimated from the simulation work. The dependence of the $k_i$ values on experimental parameters under different operating conditions is discussed in subsequent sections.

Table 5.1 Estimated intermediate blocking model plugging constant under various experimental conditions

| Operating conditions | | Intermediate blocking law of Hermia |
|---|---|---|
| | | $K_i$ ($m^{-1}$) |
| $C_o$= 6% ω=200 rpm | ΔP=150 kPa | 84.21 |
| | ΔP=250 kPa | 78.95 |
| | ΔP=350 kPa | 65.79 |
| ΔP=250 kPa $C_o$= 3% | ω=200 rpm | 78.95 |
| | ω=300 rpm | 52.63 |
| | ω=400 rpm | 47.37 |
| ΔP=250 kPa ω=300 rpm | $C_o$= 3% | 57.89 |
| | $C_o$= 6% | 60.53 |
| | $C_o$= 9% | 63.16 |

Figures 5.1 (a), (b) and (c) represent the permeate flux profile for different transmembrane pressures. For this particular study the feed concentration and stirring rate were fixed at 6% and 200 rpm, respectively. From Table 5.1 and Figure 5.1, the $k_i$ values were found to decrease with an increase in transmembrane pressure. For example, as shown in Figure 5.1, an increase in transmembrane pressure from 150 to 350 kPa resulted in a decrease in $k_i$ from 87.21-65.79$m^{-1}$. This was also observed by Sarkar (2013) for the ultrafiltration of a polysaccharide in a stirred cell. In the study the author observed that increasing the transmembrane pressure resulted in a decrease in the cake filtration constant, $k_c$, albeit marginally so. The author attributed this to the fact that the effect of pressure is marginal on the long term flux in a system whereby the cake filtration mechanism is dominating.

(a)

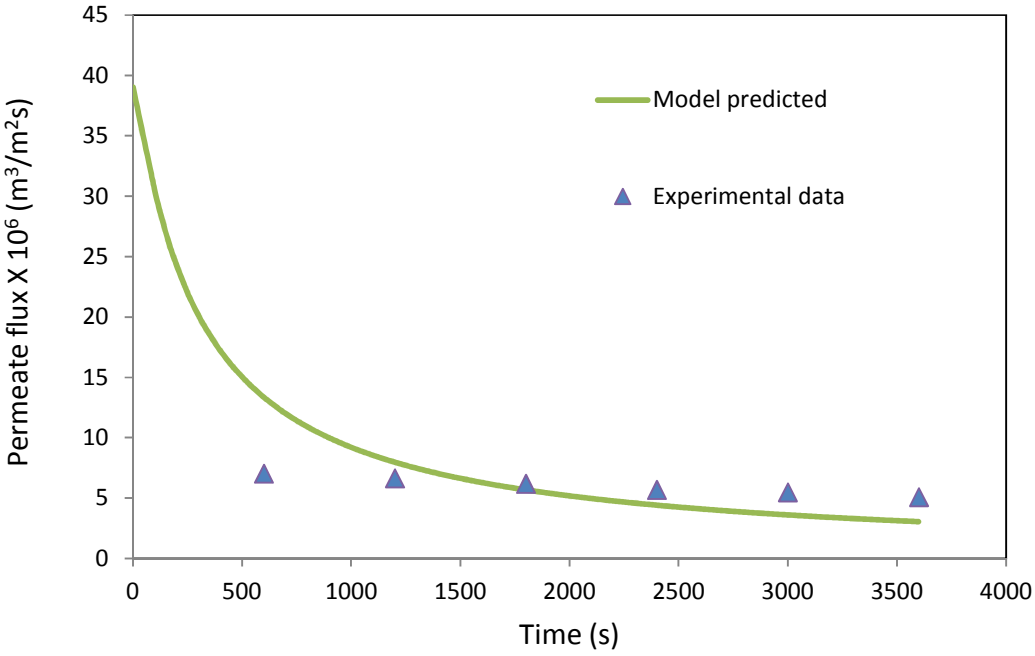
Permeate flux X 10⁶ (m³/m²s)
Time (s)
Model predicted
Experimental data
0
5
10
15
20
25
30
35
40
45
0
500
1000
1500
2000
2500
3000
3500
4000

(b)

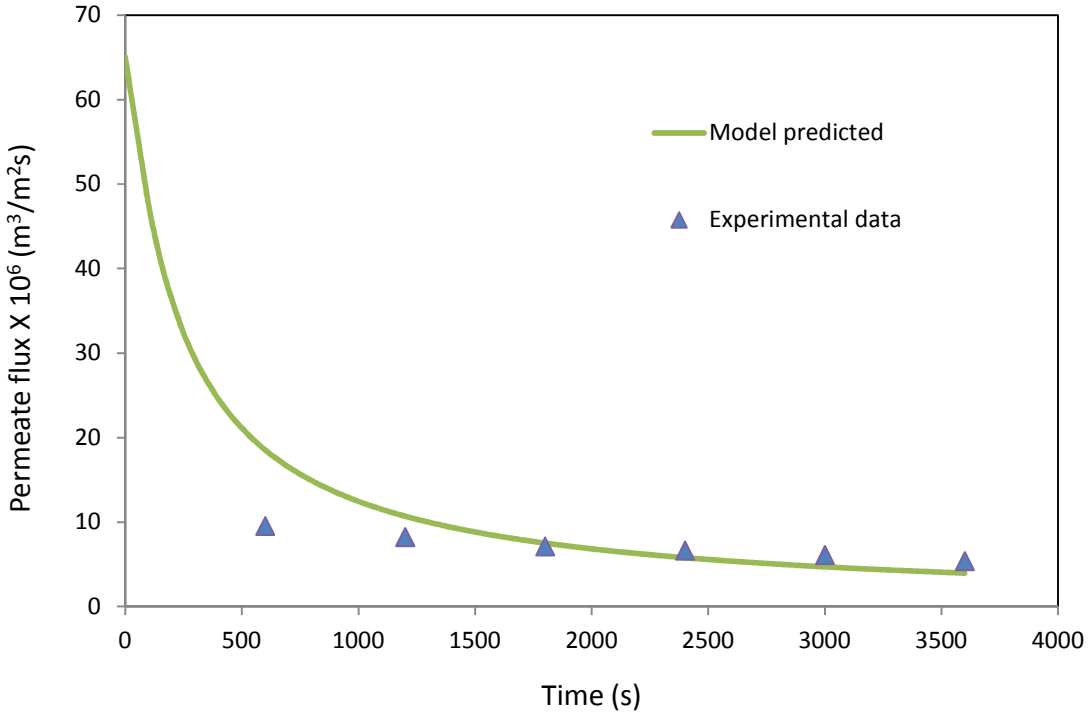
Permeate flux X 10⁶ (m³/m²s)
Time (s)
Model predicted
Experimental data
0
10
20
30
40
50
60
70
0
500
1000
1500
2000
2500
3000
3500
4000

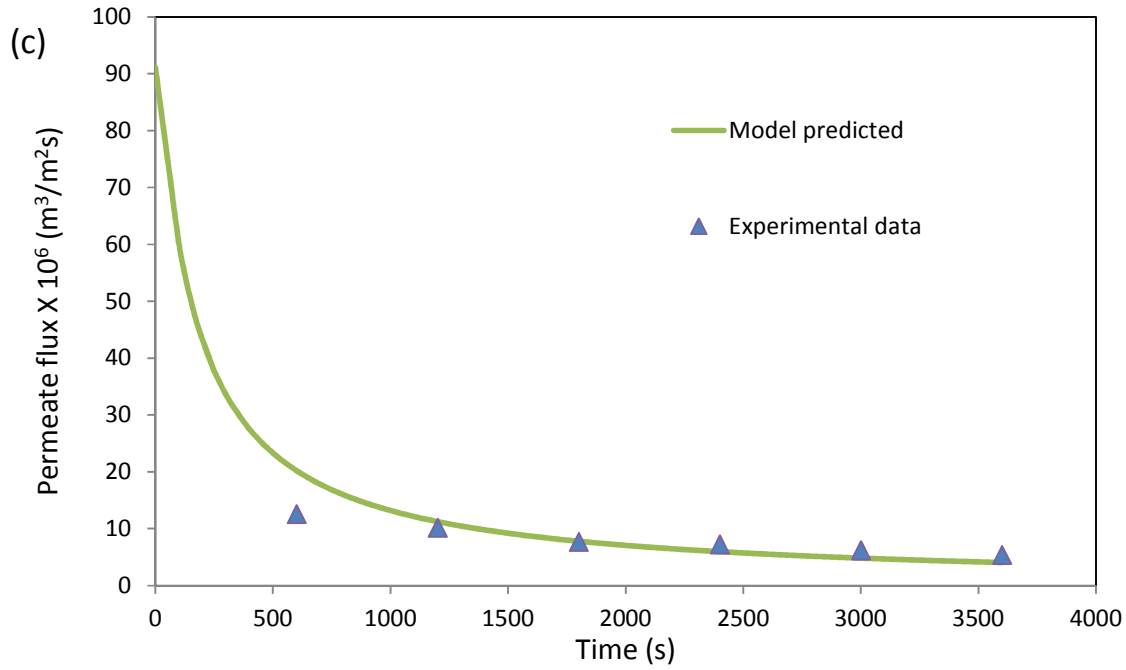


Figures 5.1 a, b and c: A graphical representation showing how the predicted $J_{cal}$ values of the intermediate blocking model fit the experimental data at different transmembrane pressures. $C_o$ = 6% and ω = 200 rpm: (a) 150 kPa, (b) 250 kPa, and (c) 350 kPa

The permeate flux profiles for different feed concentrations are shown in Figures 5.2 (a), (b) and (c) below. These are plotted for fixed transmembrane pressure and stirring rate values of 250 kPa and 300 rpm, respectively. The $k_i$ values increase with an increase in feed concentration in the range investigated. For instance, from Figure 5.2 as the feed concentration is increased from 3% to 9% (Figures 5.2 (a) and (c), respectively), the $k_i$ values increase from 57.89-63.16 $m^{-1}$. This is an indication of an increase in concentration polarization which is as a result of the increase in solute feed concentration (Sarkar, 2013).

(a)

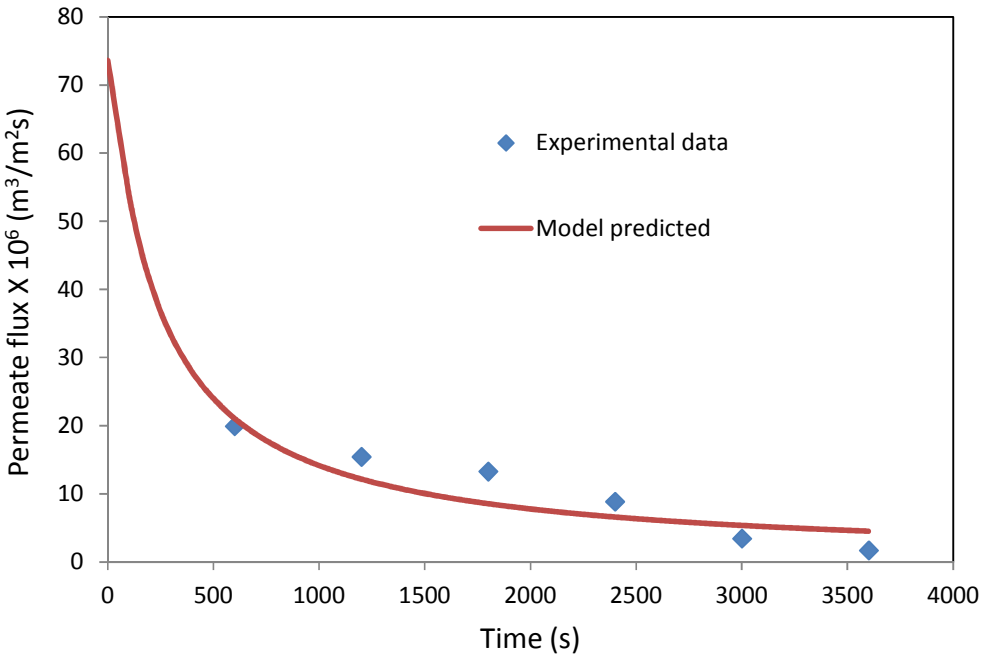
Permeate flux X 10⁶ (m³/m²s)
Time (s)
Experimental data
Model predicted
0
10
20
30
40
50
60
70
80
0
500
1000
1500
2000
2500
3000
3500
4000

(b)

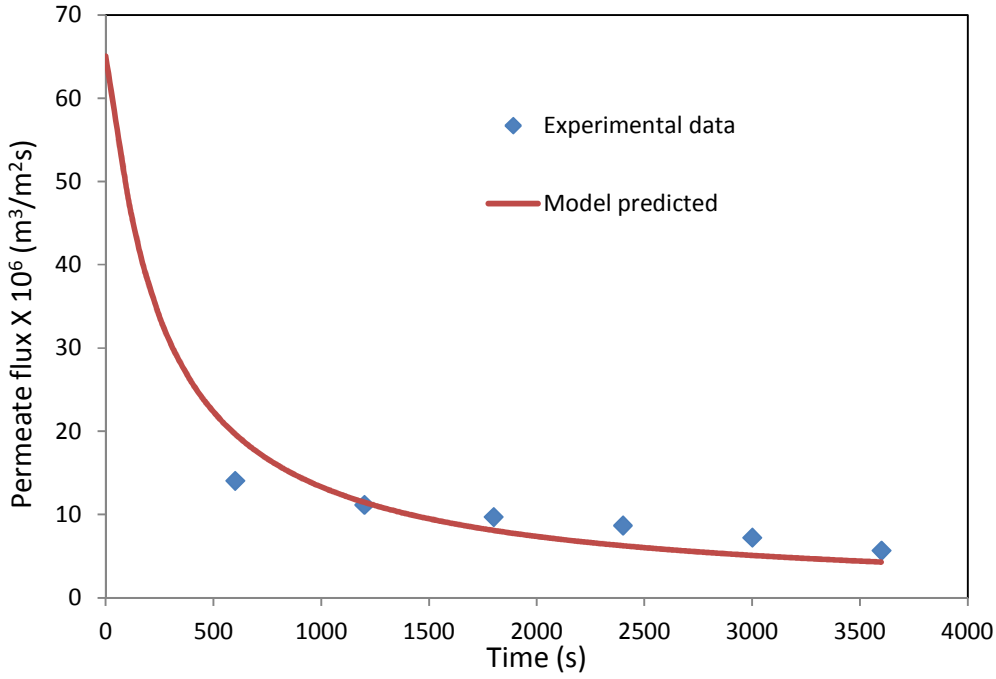
Permeate flux X 10⁶ (m³/m²s)
Time (s)
Experimental data
Model predicted
0
10
20
30
40
50
60
70
0
500
1000
1500
2000
2500
3000
3500
4000

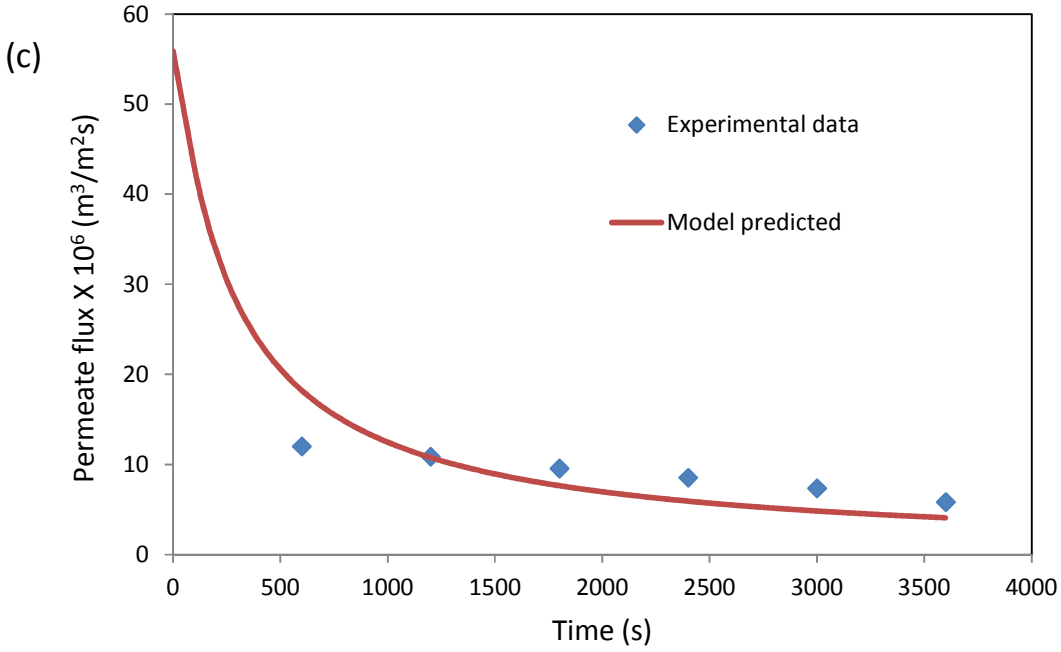


Figures 5.2 a, b and c: A graphical representation showing how the predicted $J_{cal}$ values of the intermediate blocking model fit the experimental data at different feed concentrations.

ΔP = 250 kPa and ω = 300 rpm: (a) 3%, (b) 6%, and (c) 9%

Figures 5.3 (a), (b) and (c) represent the permeate flux profiles for different stirring rates. For this study the transmembrane pressure and feed concentration values were fixed at 250 kPa and 3%, respectively. The $k_i$ values were found to decrease with an increase in stirring rate in the stirred cell. For example, in Figure 5.3, an increase in stirring rate from 200 rpm to 400 rpm led to a decrease in $k_i$ from 78.98-47.37 $m^{-1}$. This is attributed to the fact that at higher stirring rates there is enhanced turbulence close to the membrane surface which decreases concentration polarization and increases permeate flux (Sarkar, 2013).

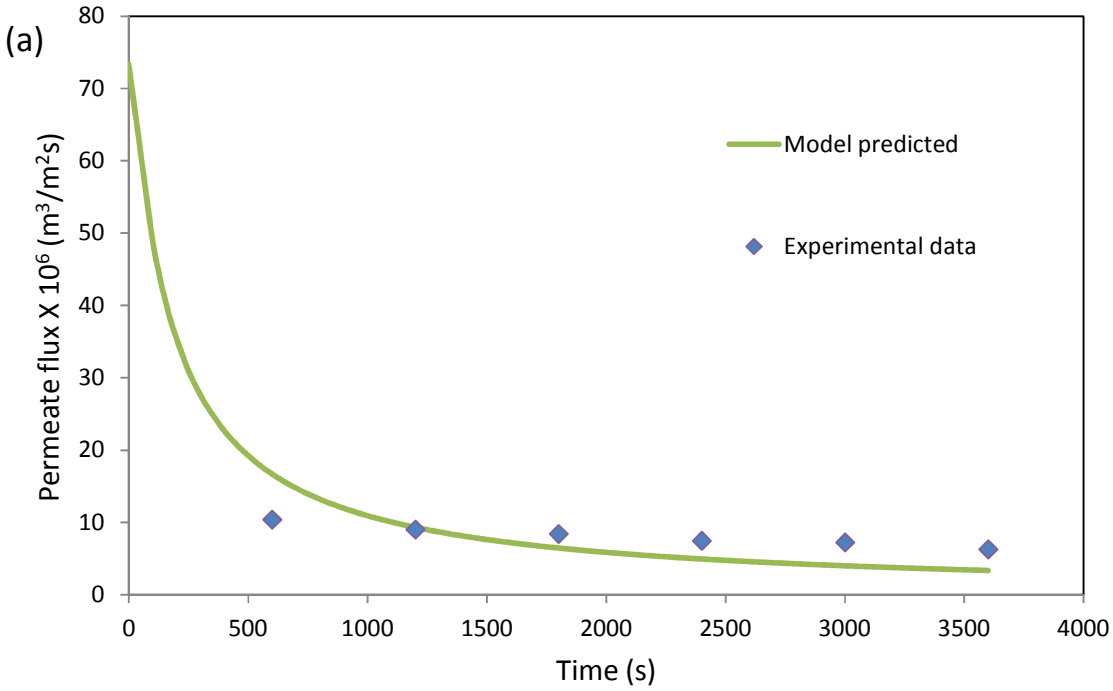
(a)
Permeate flux X 10^6 (m^3/m^2s)
Time (s)
Model predicted
Experimental data
0
10
20
30
40
50
60
70
80
0
500
1000
1500
2000
2500
3000
3500
4000

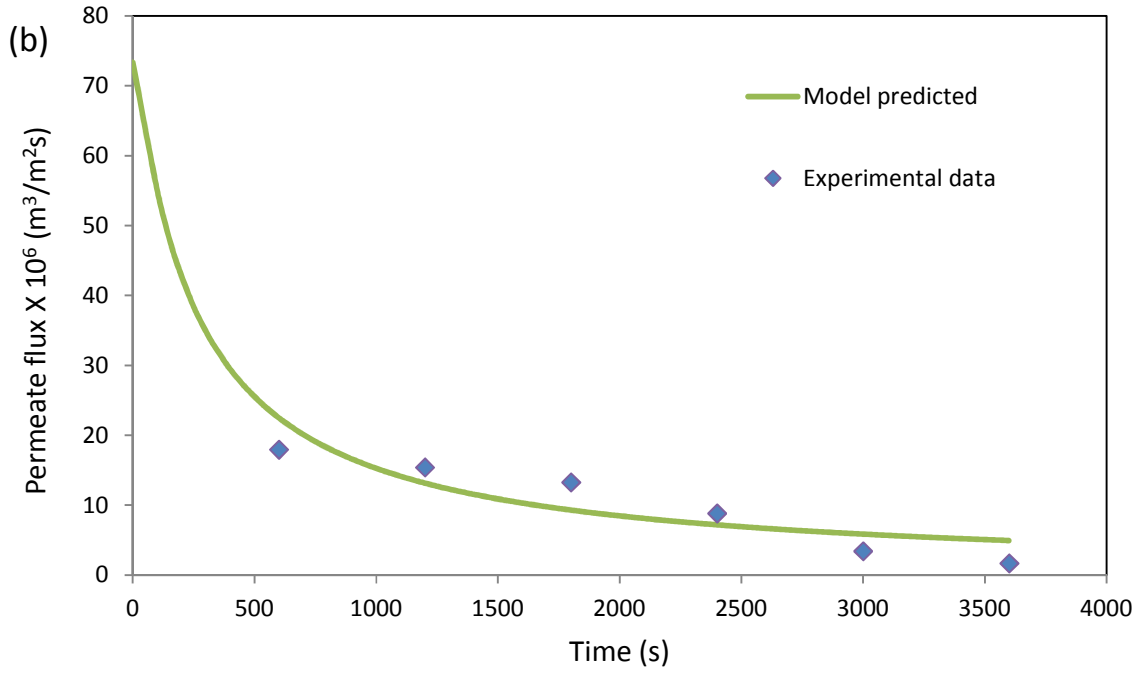
(b)
Permeate flux X 10^6 (m^3/m^2s)
Time (s)
Model predicted
Experimental data
0
10
20
30
40
50
60
70
80
0
500
1000
1500
2000
2500
3000
3500
4000

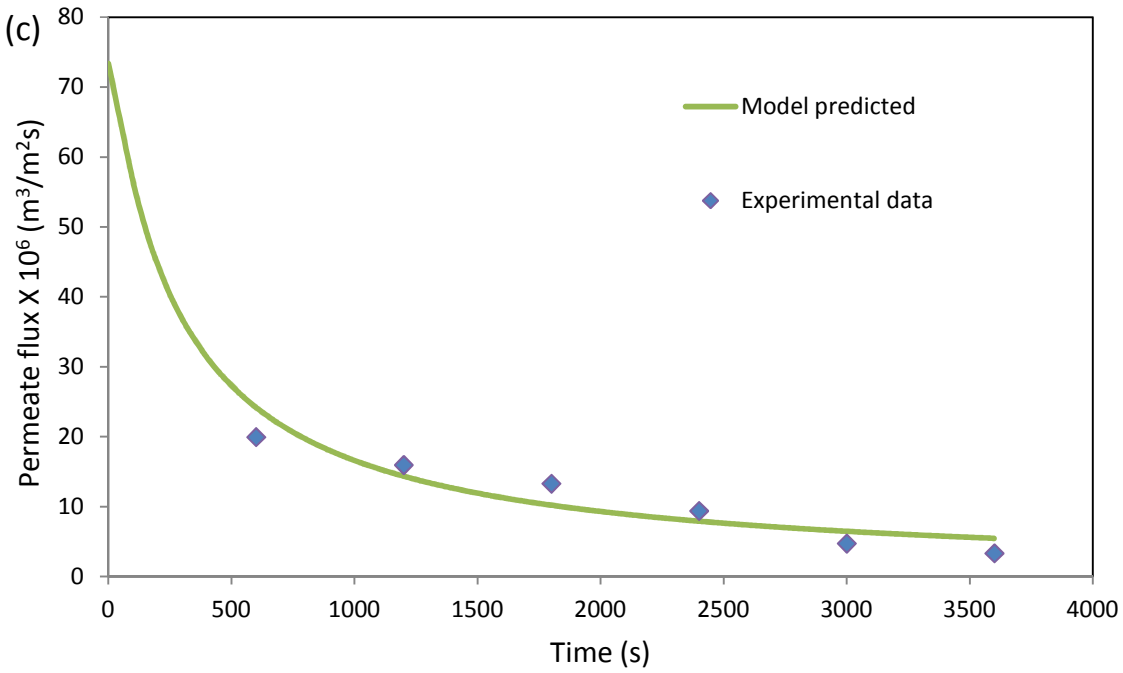


Figures 5.3 a, b and c: A graphical representation showing how the predicted $J_{cal}$ values of the intermediate blocking model fit the experimental data at different stirring rates. ΔP = 250 kPa and $C_o$ = 3%: (a) 200 rpm, (b) 300 rpm, and (c) 400 rpm

The variation of dimensionless intermediate resistance with time for different transmembrane pressures is displayed in Figure 5.4 below. For this study the feed concentration and stirring rate were fixed at 6% and 200 rpm, respectively. As shown in Figure 5.4, the dimensionless intermediate resistance increases with an increase in transmembrane pressure. At the end of the experiment the dimensionless resistance increased from 11.83 to 21.56 with a corresponding increase in transmembrane pressure from 150 to 350 kPa. This is due to the fact that there is a higher convection of solutes to the membrane surface as the transmembrane pressure is increased which leads to increased concentration polarization at the surface (Sarkar, 2013).

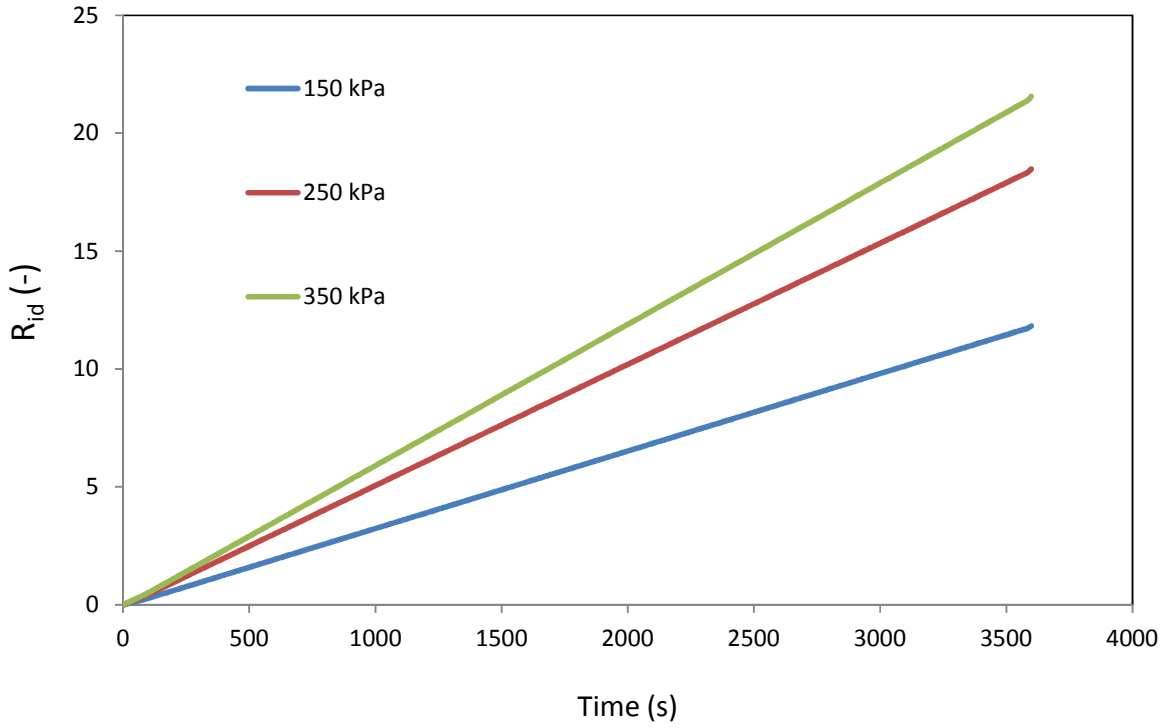


Figure 5.4 Variation of dimensionless intermediate resistance with time at different transmembrane pressure. $C_o$ = 6% and ω = 200 rpm

Figure 5.5 below represents the variation of dimensionless intermediate resistance with time at different feed concentration for fixed transmembrane pressure and stirring rate of 250 kPa and 300 rpm, respectively. An increase in the feed concentration led to an increase in the dimensionless intermediate resistance as shown in Figure 5.5. For instance, at the end of the experiment, an increase in feed concentration from 3 to 9% resulted in a corresponding increase in the dimensionless intermediate resistance from 15.28 to 16.67. A possible explanation for this observation is that in principle, an increase in feed concentration leads to a corresponding increase in concentration polarization as the fouling layer on the membrane surface is increased (Sarkar, 2013). However, it is worth noting that the effect of feed concentration on the

dimensionless intermediate resistance is marginal as compared to the effect of transmembrane pressure as shown in the preceding section.

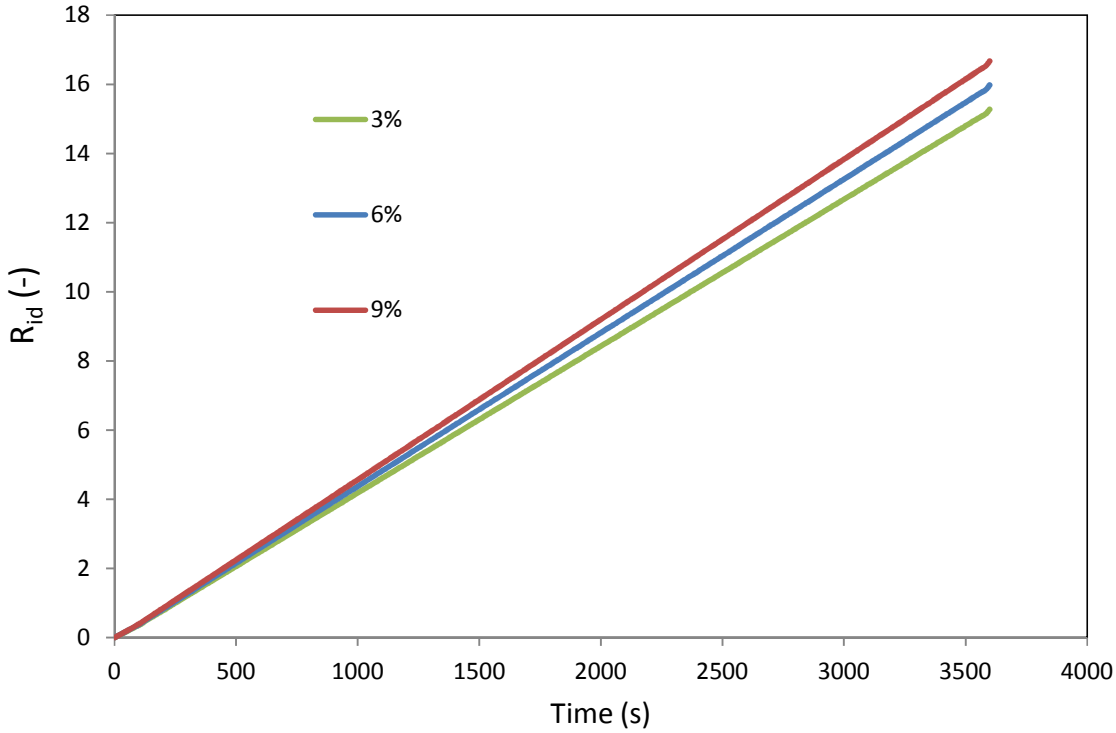


Figure 5.5 Variation of dimensionless intermediate resistance with time at different feed concentration. $\Delta P$ = 250 kPa and $\omega$ = 300 rpm

The variation of dimensionless intermediate resistance with time at different stirring rates at fixed transmembrane pressure and feed concentrations of 250 kPa and 3% is shown in Figure 5.6 below. From Figure 5.6, it can be observed that an increase in the stirring rate resulted in a decrease in the dimensionless intermediate resistance. At the end of the experiment, the intermediate resistance was reduced significantly from 20.84 to 13.89 as the stirring rate was adjusted from 200 to 300 rpm, only to be reduced marginally to 12.50 as the stirring rate was further adjusted to 400 rpm. This is because at higher stirring rates, the enhanced turbulence

close to the membrane surface assists in the mitigation of the effects of concentration polarization (Sarkar, 2013)

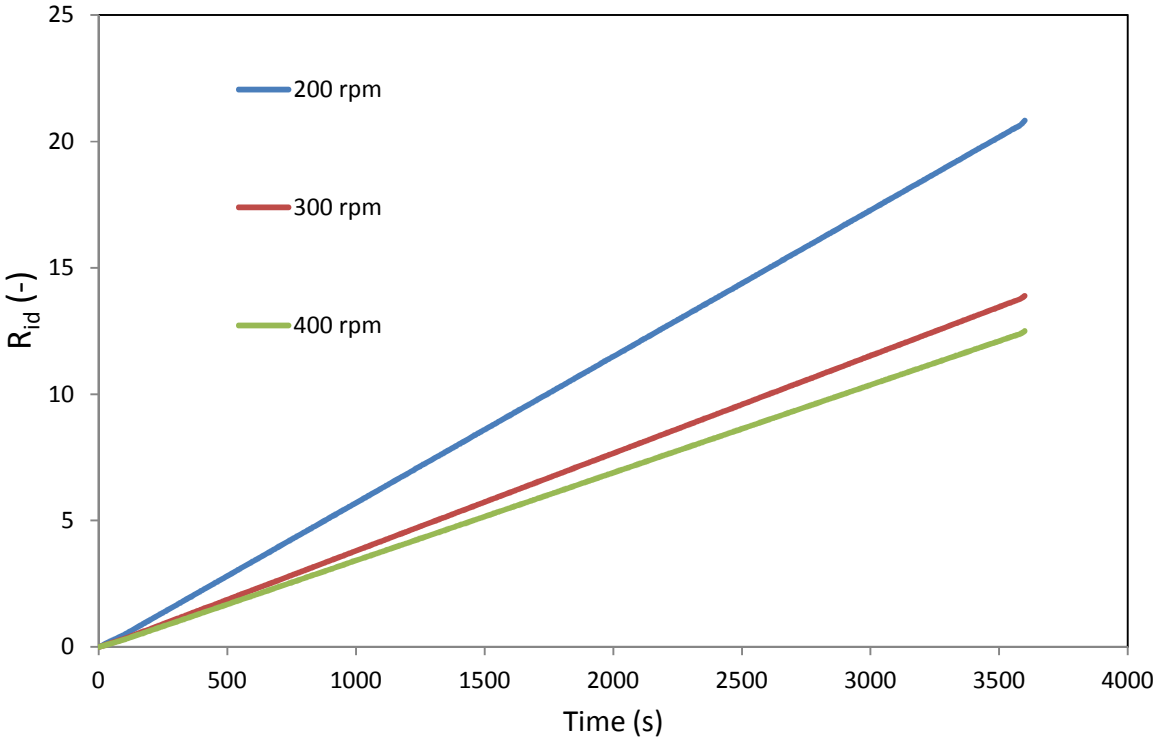


Figure 5.6 Variation of dimensionless intermediate resistance with time at different stirring rates. $\Delta P$ = 250 kPa and $C_o$ = 3%

# CHAPTER 6

## 6.1 CONCLUSIONS AND RECOMMENDATIONS

The hypothesis was proven and the objectives listed were achieved. The results showed that it is possible to extract lignin from black liquor from Kraft pulping of South African grown Eucalyptus by means of ultrafiltration. It was found that amongst the membranes investigated the highest retention of lignin was achieved using the 5 kDa membrane, which indicated that a large percentage of molecular size distribution of lignin in the black liquor sample was in the range 100-5000 Da range. Although the 5 kDa size membrane had the highest retention, its flux was too low for a comparative study. Therefore, to investigate the effect of operating parameters on both the flux and retention a 10 kDa size membrane was used.

The parameters investigated (operating pressure, feed concentration and stirring rate) had significant effects on the retention of lignin and flux. Membrane fouling was observed to have a profound negative effect on flux values in the study and the mechanisms that contributed to this were combinations of osmotic pressure build up and the development of a viscous gel layer on the membrane during operation and this was modeled using the intermediate blocking model derived from Hermia's law.

The flux decline simulation model fit experimental data for the time period 20-60 minutes. However, the model did not represent the experimental data well when the time was less than 20 minutes. The model needs to be improved to take into account the possibility of fouling being described by another mechanism such as cake filtration in addition to the intermediate mechanism is that time period.

This study should be augmented by studying the ultrafiltration of lignin in a pilot plant in a continuous mode to

- Overcome the effect of fouling associated with batch filtration
- To generate a set of data that can be applicable for ultrafiltration of black liquor on an industrial scale.

More tests can also be performed in order to

- Study the retention of lignin by ultrafiltration using ceramic membranes in a continuous pilot plant setup
- Investigate of the effects of carbonization temperature and impregnation ratio used for activation on the generation of activated carbon from lignin
- Characterize the activated carbons obtained by using lignin as a precursor and compare them to commercial samples
- Perform adsorption experiments in batch mode to adsorb copper from solution using activated carbon produced from the study to evaluate the maximum uptake and adsorption kinetics parameters

# REFERENCES

BANERJEE, S. & DE, S. (2012) An analytical solution of Sherwood number in a stirred continuous cell during steady state ultrafiltration. *Journal of Membrane Science*, 389, pp 188-196

BECHT, N.O., MALIK, D.J., & TARLETON E.S. (2008) Evaluation and comparison of protein ultrafiltration test results: Dead-end stirred cell compared with a cross-flow system. *Separation and Purification Technology*, 62, pp 228–239

BHATTACHAJEE, C. & BHATTACHARYA, P.K. (1993) Flux decline analysis in ultrafiltration of Kraft black liquor. *Journal of Membrane Science, 82*, pp 1-14

BHATTACHARJEE, C. & DATTA, S., (1997) A mass transfer model for the prediction of rejection and flux during ultrafiltration of PEG-6000. *Journal of membrane science*, 125(2), pp 303-310

BHATTACHARJEE, C. & BHATTACHARYA, P.K., (2006) Ultrafiltration of black liquor using rotating disk membrane module, *Separation and Purification Technology*, 49 (3), pp 281–290

BHATTACHARJEE, C., SARKAR, P., DATTA, S., GUPTA, B.B. & BHATTACHARYA, P.K., *Separation and Purification Technology*, 51(3), 247(2006)

BOWEN, W.R., CALVO, J.I., & HERNANDEZ, A. (1995) Steps of membrane blocking in flux decline during protein microfiltration, *Journal of Membrane Science* ,101(1-2) ,153-165

BRITZ, T. & ROBINSON, R.K., (2008) Advanced Dairy Science and Technology. John Wiley & Sons

BURANOV, A.U. & MAZZA, G., (2008) Lignin in straw of herbaceous crops, *Industrial Crops and Products*, 28, pp 237-259

CAGNON, B., PY, X., GULLIOT, A., STOECKLI, F., & CHAMBAT, G., (2009) Contributions of hemicellulose, cellulose and lignin to the mass and the porous properties of chars and steam activated carbons from various lignocellulosic precursors, *Bioresource Technology*, 100, pp 292-298

CARDOSO, M., DOMINGOS DE OLIVEIRA, É. & PASSOS, M.L. (2009) Chemical composition and physical properties of black liquors and their effects on liquor recovery operation in Brazillian pulp mills, *Fuel* 88, pp 756-763

CHAKAR, F.S. & RAGAUSKAS, A.J. (2004) Review of current and future softwood kraft lignin process chemistry, *Industrial Crops and Products* 20, pp 131-141

CHERYAN, M., (1986) Ultrafiltration handbook, Technomic Publishing Company, Inc.

DAFINOV, A., FONT, J. & GARCIA-VALLS, R. (2005) Processing of black liquors by UF/NF ceramic membranes, *Desalination*, 173, pp 83-90

DE, S. & BHATTACHARYA, P.K. (1996) Flux prediction of black liquor in cross flow ultrafiltration using low and high rejecting membranes. *Journal of Membrane Science*, 109, 109-123

DE, S., DIAS, J.M. & BHATTACHARYA, P. K. (1997) Short and long term flux decline analysis in ultrafiltration. *Chemical Engineering Communications*, 159(1), 67-89

DOHERTY, W.O.S., MOUSAVIOUN, P. & FELLOWS, C.M. (2011) value-adding to cellulosic ethanol: Lignin polymers, *Industrial Crops and Products,* 33(2), 259-276

FIERRO, V., TORNÉ-FERNÁNDEZ, V., CELZARD, A. & MONTANÉ, D. (2007) Influence of the demineriliseation on the chemical activation of Kraft lignin with orthophosphoric acid, *Journal of Hazardous Materials,* 149, pp 126-133

GONZALEZ-SERRANO, E., CORDERO, T., RODRIGUEZ-MIRASOL, J., COTORUELO, L. & RODRIQUEZ, J.J. (2004) Removal of water pollutants with activated carbons prepared from $H_3PO_4$ activation of lignin from Kraft black liquors, *Water Research* 38, pp 3043-3050

GRACE, H.P., (1956) Structure and performance of filter media, *AIChE,* 2, 307

GUO, X., ZHANG, S. & SHAN, X., (2008) Adsorption of metal ions on lignin, *Journal of Hazardous Materials* 151, pp 134-142

HAYASHI, J., KAZEHAYA, A., MUROYAMA, K. & WATKINSON, A.P., (2000) Preparation of activated carbon from lignin by chemical activation, *Carbon* 38, pp 1873-1878

HERMANS, P.H. & BREDEE, H.L., (1936) Principles of the mathematical treatment of constant-pressure filtration, *Journal of Society of Chemical Industry*, 55T, 1–11

HERMIA, J., (1982) Constant pressure blocking filtration laws—application to power-law non-Newtonian fluids, *Transaction of the Institution of Chemical Engineers*, 60, 183–187

IRITANI, E., (2013) A review on modeling of pore-blocking behaviors of membranes During pressurized membrane filtration. *Drying Technology: An International Journal*,31( 2),146-162

JOHNSON, S.T., SMITH, K.A. & DEEN, W.M. (2001) Concentration Polarization in Stirred Ultrafiltration Cells. *AIChE*, 47 (5), 1115-1125

JöNSSON, A., NORDIN, A. & WALLBERG, O. (2008) Concentration and purification of lignin in hardwood kraft pulping liquor by ultrafiltration and nanofiltration, *Chemical Engineering Research and Design* 86(11), pp 1271-1280

JöNSSON, A. & WALLBERG O. (2009) Cost estimates of Kraft lignin recovery by ultrafiltration, *Desalination* 237(1-3), pp 254-267

KIJIMA, M., HIRUKAWA, T., HANAWA, F. & HATA, T. (2011) Thermal conversion of alkaline lignin and its structured derivatives to porous carbonized materials, *Bioresource Technology* 102, pp 6279-6285

KOUTSOU, P.C. & KARABELAS, J.A. (2012) Shear stresses and mass transfer at the base of a stirred filtration cell and corresponding conditions in narrow channels with spacers. *Journal of Membrane Science*, 399– 400, pp60– 72

KRIAA, A., HAMDI, N. & SRASRA, E. (2010) Removal of Cu (II) from water pollutant with Tunisian activated lignin prepared by phosphoric acid activation, *Desalination* 250, pp 179-187

KUBO, S., URAKI, Y. & SANO, Y. (1998) Preparation of carbon fibers from softwood lignin by atmospheric acetic acid pulping, *Carbon* 36, pp 1119-1124

LYKO, H., DEERBERG, G. & WEIDNER, E. (2009) Coupled production in biorefineries-Combined use of biomass as a source of energy, fuels and materials, *Journal of Biotechnology,* 142, pp 78-86

MARINOVA, M., MATEOS-ESPEJEL, E., JEMAA, N. & PARIS, J. (2009) Addressing the increased energy demand of a Kraft mill biorefinery: The hemicellulose extraction case, *Chemical Engineering Research and Design,* 87, pp 1269-1275

MONDOR, M., GIRARD, B. & MORESOLI, C. (2000) Modeling flux behavior for membrane filtration of apple juice. *Food Research International*, 33(7), 539-548

MONTANÉ, D., TORNÉ-FERNÁNDEZ, V. & FIERRO, V. (2005) Activated carbons from lignin: kinetic modelling of the pyrolysis of Kraft lignin activated with phosphoric acid, *Chemical Engineering Journal* 106, pp 1-12

MOSHKELANI, M., MARINOVA, M., PERRIER, M. & PARIS, J. (2012) The forest biorefinery and its implementation in the pulp and paper industry: Energy overview, *Applied Thermal Engineering*, 50(2), 1427

MUGISIDI, D., RANALDO, A., SOEDARSONO, J. W. & HIKAM, M. (2007) Modification of activated carbon using sodium acetate and its regeneration using sodium hydroxide for the adsorption of copper from aqueous solution, *Carbon* 45**,** pp 1081-1084.

NICOLAS, S., BALANNEC, B., BELINE, F. & BARIOU, B. (2000) Ultrafiltration and reverse osmosis of small non-charged molecules: a comparison study of rejection in a stirred and an unstirred batch cell. *Journal of Membrane Science*, 164, pp 141–155

NOORDMAN, T. R., KETELAAR, T. H., DONKERS, F., & WESSELINGH, J. A. (2002) Concentration and desalination of protein solutions by ultrafiltration. *Chemical Engineering Science*, 57, pp693 – 703

NZIHOU, A. (2010) Toward the valorization of waste and biomass, *Waste Biomass Valorization* 1, pp 3-7

PANDEY, M.P. & KIM, C.S. (2011) Lignin depolymerization and conversion: A review of thermochemical methods, *Chemical Engineering Technology* 34, pp 29-41

SARKAR, D., BHATTACHARYA, A. & BHATTACHARJEE, C. (2010) Modeling the performance of a standard single stirred ultrafiltration cell using variable velocity back transport flux. *Desalination*, 261, pp89–98

SARKAR. B. (2013) A combined complete pore blocking and cake filtration model during ultrafiltration of polysaccharide in a batch cell, *Journal of Food Engineering*, 116, 333-343

SATYANARAYANA, S.V., BHATTACHARYA, P.K. & DE, S. (2000) Flux decline during ultrafiltration of kraft black liquor using different flow modules: a comparative study. *Separation and Purification Technology*, 20(2-3), pp155–167

SCHWARZE, M., LE, D.K., WILLE, S., DREWS, A., ARLT, W. & SCHOMÄCKER, R. (2010) Stirred cell ultrafiltration of aqueous micellar TX-100 solutions. *Separation and Purification Technology*, 74(1), pp 21–27

SIXTA, H., SCHILD, G. (2009) A new generation Kraft process, *Lenzinger Berichte* 87, pp 26-37

SUHAS, CARROTT, P.J.M., CARROTT, M.M.L. (2007) Lignin-from natural adsorbent to activated carbon: A review, *Bioresource Technology* 98, pp 2301-2312

SUN, R. & TOMKINSON, J. (2001) Fractional separation and physico-chemical analysis of lignins from the black liquor of oil palm trunk fibre pulping, *Separation and Purification Technology* 24, pp 529-539

TOLEDANO, A., GARCÍA, A., MONDRAGON, I. & LABIDI, J. (2010) Lignin separation and fractionation by ultrafiltration, *Separation and Purification Technology* 71, 38-43

TOLEDANO, A., SERRANO, L., GARCIA, A., MONDRAGON, I. & LABIDI, J. (2010) Comparative study of lignin fractionation b ultrafiltration and selective precipitation, *Chemical Engineering Journal*, 157, pp 93-99

VAN HAZENDONK, J.M., REINERINK, J.M.E., DE WAARD, P., VAN DAM, J.E.G., (1996) Structural analysis of acetylated hemicellulose polysaccharides from fibre flax ( *Linum usitatissimum L.*), *Carbohydrate Research*, 291, pp 141-154

WALLBERG, O., HOLMQVIST, A. & JöNSSON, A. (2005) Ultrafiltration of Kraft cooking liquors from a continuous cooking process, *Desalination*, 180(1-3), pp 109-118

WALLBERG, O. & JöNSSON, A. (2006) Separation of lignin in kraft cooking liquor from a continuous digester by ultrafiltration at temperatures above 100$^{o}$C, *Desalination* 195(1-3), pp 187-200

WALLBERG, O., JöNSSON, A. & WIMMERSTEDT, R. (2003) (a) Fractionation and concentration of kraft black liquor lignin with ultrafiltration, *Desalination* 154, pp 187-199

WALLBERG, O., JöNSSON, A., WIMMERSTEDT, R. (2003) (b) Ultrafiltration of kraft liquor with a ceramic membrane, *Desalination* 156, pp 145-153

WALLBERG, O., LINDE, M. & JöNSSON, A. (2006) Extraction of lignin and hemicelluloses from kraft black liquor, *Desalination* 199, pp 413-414

XIAO, K., SHEN, Y. & HUANG, X. (2013) An analytical model for membrane fouling evolution associated with gel layer growth during constant pressure stirred dead-end filtration. *Journal of Membrane Science*, 427, 139-149

YIN, C. Y., AROUA, M. K. & DAUD, W. M. A. W. (2007) Impregnation of palm shell activated carbon with polyethyleneimine and its effects on $Cd^{2+}$ adsorption, *Colloids and Surfaces* 307**,** pp 128-136.

# APPENDIX A

# LIST OF PROJECT OUTPUTS

- A poster titled ‘’Ultrafiltration and valorisation of lignin in black liquor from South African Kraft mills: A case study of activated carbon generation and its application’’ was presented at the 2013 TAPPSA National Conference & Exhibition, October 22-23, 2013, Durban, South Africa

- A poster titled ‘’Ultrafiltration and valorisation of lignin in black liquor from South African Kraft mills: A focus on dead-end stirred cell filtration’’ was presented at the 2014 ICCT/SAIChE joint conference. The International Association of Chemical Thermodynamics (IACT) and the South African Institution of Chemical Engineers (SAIChE) jointly hosted the International Conference on Chemical Thermodynamics (ICCT) and the SAIChE National Conference from 27 July 2014 to 1 August 2014 at the Durban International Convention Centre in Durban, South Africa.

- A manuscript titled “Stirred cell ultrafiltration of lignin from black liquor generated from South African Kraft mills " is in preparation to be submitted in a peer-reviewed journal for publication

- A manuscript tilted ‘’ Ultrafiltration of lignin from black liquor: Modelling of decline in flux’’ is in preparation to be submitted in a peer-reviewed journal for publication